

# Time-Optimal Control for High-Order Chain-of-Integrators Systems with Full State Constraints and Arbitrary Terminal States (Part I, Extended Version)

Yunan Wang, Chuxiong Hu, *Senior Member, IEEE*, Zeyang Li, Shize Lin, Suqin He, Ze Wang, *Member, IEEE*, and Yu Zhu, *Member, IEEE*

**Abstract**—Time-optimal control for high-order chain-of-integrators systems with full state constraints and arbitrary given terminal states remains a challenging problem in the optimal control theory domain, yet to be resolved. To enhance further comprehension of the problem, this paper establishes a novel notation system and theoretical framework, providing the switching manifold for high-order problems in the form of switching laws. Through deriving properties of switching laws on signs and dimension, this paper proposes a definite condition for time-optimal control. Guided by the developed theory, a trajectory planning method named the manifold-intercept method (MIM) is developed. The proposed MIM can plan time-optimal jerk-limited trajectories with full state constraints, and can also plan near-optimal non-chattering higher-order trajectories with negligible extra motion time compared to optimal profiles. Numerical results indicate that the proposed MIM outperforms all baselines in computational time, computational accuracy, and trajectory quality by a large gap.

**Index Terms**—Optimal control, linear systems, variational methods, switched systems, trajectory planning.

## I. INTRODUCTION

HIGH-ORDER chain-of-integrators systems have been universally utilized in computer numerical control (CNC) machining [1], [2], robotic motion control [3], [4], [5], semiconductor device fabrication [6], [7], and autonomous driving [8]. Trajectory planning has a significant influence on motion efficiency and accuracy in those scenarios [9], [10]. However, time-optimal control for high-order chain-of-integrators systems with full state constraints and arbitrary terminal states remains a challenging and significant open problem in the optimal control theory domain, yet to be resolved.

The time-optimal control problem for chain-of-integrators requires planning a trajectory with minimum motion time from a given initial state vector to a terminal state vector, where the system state vector is composed of components such as position, velocity, acceleration, and so forth. State constraints require that all system state components are limited by given upper bounds, while the initial states and the terminal states are specified arbitrarily. A fifth order trajectory planned by the proposed Algorithm 1 is shown in Fig. 1. The input

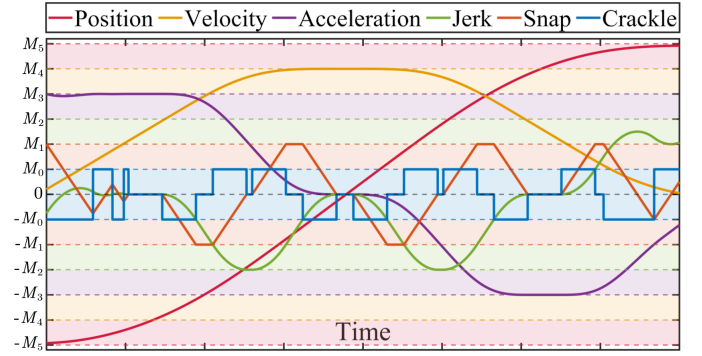


Fig. 1. A fifth order trajectory planned by the proposed method.  $M_5$ ,  $M_4$ ,  $M_3$ ,  $M_2$ ,  $M_1$ , and  $M_0$  are the upper bounds of position, velocity, acceleration, jerk, snap, and crackle, respectively. The trajectory can be represented as  $00(3,2)000301020104010201030100$  in this paper.

control, i.e., crackle, and the system states, i.e., position, velocity, acceleration, jerk, and snap, are bounded by the given constraints. The control is always maximum, minimum, or zero along the planned trajectory, satisfying the Bang-Singular-Bang control law [11].

In optimal control, numerous research has been conducted on time-optimal control for chain-of-integrators. The problem with only input saturation has been fully solved based on Pontryagin's maximum principle (PMP) [12], where theorems on the Bang-Bang control [13] and the analytic expression of the optimal control [14] are well-known. Marchand et al. [15] proposed a discrete-time control law based on the above problem. However, the time-optimal problem with input saturation and full state constraints remains unsolved, especially when the initial and terminal states are arbitrarily given, i.e., the terminal states are allowed to be non-zero. The 2nd order problem is trivial [16], but 3rd or higher-order problems have not been solved well. Haschke et al. [17] proposed an online time-optimal jerk-limited trajectory planning method without position constraints. Kröger [18] developed the Reflexxes type IV motion library, solving the third order problem without given terminal acceleration and position constraints. Berscheid and Kröger [19] fully considered third order chain-of-integrators with arbitrary terminal states and no position constraints, resulting in a widely-used jerk-limited trajectory planning package, i.e., Ruckig. Some approaches

Corresponding author: Chuxiong Hu (e-mail: cxhu@tsinghua.edu.cn). The authors are all with the Department of Mechanical Engineering, Tsinghua University, Beijing 100084, China.

on continuous path following time-optimal trajectory planning are proposed in [20], with an order lower than 3. To the best of our knowledge, there has been no mature method available for planning 4th order optimal trajectories with full state constraints so far.

For higher-order problems, the control invariant set [21] and the switching surface [22] are significant tools, which provide the nature of the time-optimal problem [23]. Mitchell et al. [24] calculated the invariant set based on level sets of solutions of a partial differential equation. Tahir et al. [25] employed a polyhedral approximation to characterize the invariant set. Doeser et al. [26] constructed the third order invariant sets for integrators. Yury [27] obtained the switching surface for the 3rd order problem in part. He et al. [11] provided the explicitly analytic expressions of the complete switching surfaces for the 3rd order problem with zero terminal states. However, the investigation of switching surfaces for 3rd order problems remains incomplete, while limited studies on switching manifold have been conducted for 4th order or higher-order problems. Specifically, the existence of chattering phenomena [28], i.e., the control switching for infinite times in a finite time period, still remains unknown in the investigated problem, let alone optimal control.

Since higher-order problems are lack of theoretical results, scholars either discretize the continuous-time problem and solve the discrete problem by numerical optimization, or plan feasible-but-not-optimal trajectories in engineering. Direct methods have been widely applied in numerical optimal control problems, and some optimization solvers have been built, such as CasADi [29], ICLOCS2 [30], and Yop [31]. However, the time-optimal control problem in the 4th or higher-order is non-convex in discrete time, leading to high computational time and failure in obtaining optimal solutions. Leomanni et al. [32] transformed the time-optimal problem into sequential convex optimization problems, but the resulting trajectory exhibits serious oscillations. Solving the time-optimal problem for high-order chain-of-integrators systems efficiently and accurately is still challenging.

Quasi-optimal trajectories, especially in the S-curve form, are widely used in industry. Erkorkmaz et al. [33] applied jerk-limited trajectories in the S-curve form in high-speed CNC machining. Dai et al. [34] planned snap-limited trajectories by solving motion time in S-curves. Ezair et al. [35] proposed a greedy recursive trajectory planning method for the high-order problem with full state constraints, but the method would fail for cases where the terminal position is close to the initial position, and the terminal velocity is far from the initial velocity. Oland et al. [36] planned suboptimal 4th order trajectories without any constraints to obtain a zero terminal based on exponential activation functions. However, the current methods either underutilize the inertia of system states or fall short of attaining full state constraints, thereby leading to unsatisfactory in motion time.

This paper theoretically studies the time-optimal control problem for high-order chain-of-integrators systems with full state constraints and arbitrary initial as well as terminal states. A novel notation system and theoretical framework is established in Section III, providing key concepts, i.e., the

switching law and the optimal-trajectory manifold. A trajectory planning method named the manifold-intercept method (MIM) is proposed in Section IV. In Part II [37], chattering of the problem is investigated. The contributions of this paper include the following aspects:

- 1) This paper establishes a novel notation system and theoretical framework for the classical and longstanding problem in optimal control, i.e., the time-optimal control problem for high-order chain-of-integrators systems. Through comprehensive analysis of states and costates, the framework can provide the switching manifold for high-order problems in the form of switching laws. Notably, limited studies on the switching hypersurface have been conducted even for 4th order problems. This paper derives properties of switching laws on signs as well as dimension and proposes a definite condition of augmented switching laws, imposing a necessary-and-stricter condition on optimal control compared to the Bellman's principle of optimality.
- 2) Guided by the developed framework, this paper proposes an efficient trajectory planning algorithm called manifold-intercept method (MIM). The proposed MIM can plan near-time-optimal trajectories for 4th or higher-order problems with only negligible extra motion time compared to time-optimal trajectories, avoiding chattering in high-order problems with quasi-optimal terminal time compared to optimal solutions. Specifically, under a set of typical kinematic parameters for the ultra-precision wafer stage, the trajectory planned by the proposed MIM achieves only 0.14% relative error of terminal time compared to the optimal trajectory with chattering. The proposed MIM outperforms all baselines on computational time, computational accuracy, and trajectory quality by a large gap. To the best of our knowledge, there has been no mature method available for planning 4th order optimal trajectories with full state constraints so far.
- 3) For 3rd order problems, the proposed MIM can plan strictly time-optimal trajectories with full state constraints. According to the available literature, the proposed MIM is the first 3rd order trajectory planning method with full state constraints and arbitrary terminal states. While it is claimed that Ruckig in pro version [38] can achieve 3rd order trajectories with full state constraints, it is neither open-source nor explicit publishes its underlying principles. Since 3rd order trajectories are widely applied in the industry [1], [26], the proposed algorithm has significant application value.

## II. PROBLEM FORMULATION

As mentioned in Section I, time-optimal control for chain-of-integrator systems is a classical problem in the optimal control theory domain, remaining challenging to plan trajectories with input saturation, full state constraints [11], and arbitrary terminal states [18], [19]. Generally, the problem can

be summarized as

$$\min J = \int_0^{t_f} dt = t_f, \quad (1a)$$

$$\text{s.t. } \dot{\mathbf{x}}(t) = \mathbf{A}\mathbf{x}(t) + \mathbf{B}u(t), \forall t \in [0, t_f], \quad (1b)$$

$$\mathbf{x}(0) = \mathbf{x}_0, \mathbf{x}(t_f) = \mathbf{x}_f, \quad (1c)$$

$$|x_k(t)| \leq M_k, \forall t \in [0, t_f], k = 1, 2, \dots, n, \quad (1d)$$

$$|u(t)| \leq M_0, \forall t \in [0, t_f], \quad (1e)$$

where  $\mathbf{x} = (x_1, x_2, \dots, x_n) \in \mathbb{R}^n$  is the state vector of the system,  $u \in \mathbb{R}$  is the control input.  $\mathbf{x}_0 = (x_{01}, x_{02}, \dots, x_{0n})$  and  $\mathbf{x}_f = (x_{f1}, x_{f2}, \dots, x_{fn})$  are the assigned initial state vector and terminal state vector.  $n$  is called the order of problem (1). The notation  $(\bullet)$  means  $[\bullet]^\top$ . In (1),

$$\mathbf{A} = \begin{bmatrix} 0 & \cdots & 0 & 0 \\ 1 & \cdots & 0 & 0 \\ \vdots & \ddots & \vdots & \vdots \\ 0 & \cdots & 1 & 0 \end{bmatrix} \in \mathbb{R}^{n \times n}, \mathbf{B} = \begin{bmatrix} 1 \\ 0 \\ \vdots \\ 0 \end{bmatrix} \in \mathbb{R}^n. \quad (2)$$

In other words,  $\dot{x}_1 = u$ , and  $\forall 1 \leq k < n, \dot{x}_{k+1} = x_k$ .

Problem (1) possesses a clear physical significance. For example, if  $n = 4$ ,  $x_4, x_3, x_2, x_1$ , and  $u$  are the position, velocity, acceleration, jerk, and snap of a 1-axis motion system, respectively. Then, (1) requires planning a trajectory with minimum motion time from a given initial state vector to a terminal state vector under box constraints.

For convenience, denote  $\mathbf{M} = (M_0, M_1, \dots, M_n) \in \mathbb{R}_{++} \times \mathbb{R}_{++}^n$ , where  $\mathbb{R}_{++} = \mathbb{R}_{++} \cup \{\infty\}$  is the strictly positive part of the extended real number line.  $M_k = \infty$  if  $x_k$  is unconstrained. Problem (1) is denoted as  $\mathcal{P}(\mathbf{x}_0, \mathbf{x}_f; \mathbf{M})$ .

In order to solve the optimal control problem (1), the Hamiltonian is constructed as

$$\begin{aligned} \mathcal{H}(\mathbf{x}(t), u(t), \lambda_0, \boldsymbol{\lambda}(t), \boldsymbol{\eta}(t), t) \\ = \lambda_0 + \lambda_1 u + \sum_{k=2}^n \lambda_k x_{k-1} + \sum_{k=1}^n \eta_k (|x_k| - M_k), \end{aligned} \quad (3)$$

where  $\lambda_0 \geq 0$ .  $\boldsymbol{\lambda}(t) = (\lambda_1(t), \lambda_2(t), \dots, \lambda_n(t)) \in \mathbb{R}^n$  is the costate vector, and  $(\lambda_0, \boldsymbol{\lambda}(t)) \neq 0$ .  $\boldsymbol{\lambda}$  satisfies the Euler-Lagrange equations [39]:

$$\dot{\lambda}_k = -\frac{\partial \mathcal{H}}{\partial x_k}, k = 1, 2, \dots, n, \quad (4)$$

i.e.,

$$\begin{cases} \dot{\lambda}_k = -\lambda_{k+1} - \eta_k \operatorname{sgn}(x_k), k < n, \\ \dot{\lambda}_n = -\eta_n \operatorname{sgn}(x_n). \end{cases} \quad (5)$$

The initial costates  $\boldsymbol{\lambda}(0)$  and the terminal costates  $\boldsymbol{\lambda}(t_f)$  are not assigned since  $\mathbf{x}(0)$  and  $\mathbf{x}(t_f)$  are given in problem (1).

In (3),  $\boldsymbol{\eta}$  is the multiplier vector induced by inequality constraints (1d), satisfying

$$\eta_k \geq 0, \eta_k (|x_k| - M_k) = 0, k = 1, 2, \dots, n. \quad (6)$$

Equivalently,  $\forall t \in [0, t_f]$ ,  $\eta_k(t) \neq 0$  only if  $|x_k(t)| = M_k$ .

PMP gives the results that the input control  $u(t)$  minimizes the Hamiltonian  $\mathcal{H}$  [12], i.e.,

$$u(t) \in \arg \min_{|U| \leq M_0} \mathcal{H}(\mathbf{x}(t), U, \lambda_0, \boldsymbol{\lambda}(t), \boldsymbol{\eta}(t), t). \quad (7)$$

Therefore,

$$u(t) = \begin{cases} M_0, & \lambda_1(t) < 0 \\ *, & \lambda_1(t) = 0, \\ -M_0, & \lambda_1(t) > 0 \end{cases} \quad (8)$$

where  $u(t)$  is undetermined during  $\lambda_1(t) = 0$ . Evidently, the value of  $u(t)$  in a zero-measure set have no influence on the integral result. However, a singular condition occurs when  $\lambda_1(t) = 0$  holds for a period of time. The control law for the 3rd order version of (8) was previously reasoned and named the Bang-Singular-Bang time-optimal control law in [11].

The continuity of the system is guaranteed in two folds. On one hand,

$$\forall t \in [0, t_f], \mathcal{H}(\mathbf{x}(t), u(t), \lambda_0, \boldsymbol{\lambda}(t), \boldsymbol{\eta}(t), t) \equiv 0 \quad (9)$$

holds along the time-optimal trajectory. On the other hand, the junction condition [12] is induced as a guarantee of (9). More specifically,  $\boldsymbol{\lambda}$  might jump when the state vector  $\mathbf{x}$  enters or exits the boundaries of the inequality constraints (1d). In other words,  $\boldsymbol{\lambda}$  might not be continuous when  $\mathbf{x}$  switches between  $|x_k| < M_k$  and  $|x_k| = M_k$  for some  $k$ .

### III. SYSTEM BEHAVIOR ANALYSIS AND SWITCHING LAWS FOR THE TIME-OPTIMAL CONTROL PROBLEM

Section II has provided the problem form and some properties of system states and costates. The Bang-Singular-Bang control law (8) indicates the importance of the costate analysis. Section III-A and Section III-B analyze costates and system behaviors, respectively. Then, system behaviors of problem (1) are classified into finite ones and the theory of the switching law is developed in Section III-C. Finally, the definite condition of problem (1) is induced by the proposed augmented switching law in Section III-D.

#### A. Jump Condition of Costates $\boldsymbol{\lambda}$

As mentioned in Section II, the costate vector  $\boldsymbol{\lambda}$  might not be continuous at the connection of unconstrained arcs and constrained boundary, i.e.,  $|x_k|$  increases onto  $M_k$  or decreases from  $M_k$  for some  $k$ . The above behavior is called the junction condition (or jump condition) of costates [40]. The junction condition has a significant influence on the switching law of the optimal control  $u$ .

Assume the junction condition for  $|x_k| \leq M_k$  occurs at time  $t_1$ . According to [40],  $\exists \mu \leq 0$ , s.t.

$$\boldsymbol{\lambda}(t_1^+) - \boldsymbol{\lambda}(t_1^-) = \mu \frac{\partial (|x_k| - M_k)}{\partial \mathbf{x}} = \mu \operatorname{sgn}(x_k) \mathbf{e}_k, \quad (10)$$

where the  $k$ -th component of  $\mathbf{e}_k \in \mathbb{R}^n$  is 1, and other components of  $\mathbf{e}_k$  are 0. In other words,  $\forall i \neq k, \lambda_i$  is continuous at  $t_1$ , while  $\lambda_k$  might jump at  $t_1$ .

Two cases for the junction condition exist where (a)  $|x_k| \equiv M_k$  for a period of time, i.e., the connection of an unconstrained arc and a constrained arc, and where (b)  $|x_k|$  touches  $M_k$  at a single time point i.e., the connection of two unconstrained arcs at the constrained boundary. The above two cases will be discussed in Section III-A1 and Section III-A2. Among them, Case 1 induces the system

behavior defined in Definition 1, while Case 2 induces the tangent marker in Definition 8. The limit point of chattering phenomena in problem (1), in any one-sided neighborhood of which  $|x_k| = M_k$  and  $|x_k| < M_k$  occur for infinite times, will be investigated in Part II of this work [37].

1) *Case 1.  $|x_k| \equiv M_k$  for A Period of Time:*

Without loss of generality, assume that  $\forall t \in [t_1, t_2]$ ,  $x_k(t) \equiv M_k$ , and  $\exists \delta > 0$ ,  $\forall t \in (t_1 - \delta, t_1)$ ,  $x_k(t) < M_k$ . The case where  $x_k$  leaves  $M_k$  or  $x_k \equiv -M_k$  can be reasoned similarly.

During  $t \in [t_1, t_2]$ ,  $x_k \equiv M_k$ ,  $\dot{x}_1 = u$ , and  $\forall i < k$ ,  $\dot{x}_{i+1} = x_i$ . Hence,  $u \equiv 0$  and  $\forall i < k$ ,  $x_i \equiv 0$ . Note that  $\forall i > k$ ,  $x_i(t)$  is a polynomial of degree  $(i - k)$ , and  $\left| \frac{d^{(i-k)} x_i}{dt^{(i-k)}} \right| \equiv M_k \neq 0$ . So  $|x_i| = M_i$  holds at most at  $2(i - k)$  number of points. In other words,  $\forall i > k$ ,  $|x_i| < M_i$  holds except at finite time points. From (6) and (8),  $\lambda_1 \equiv 0$ , and  $\forall i \neq k$ ,  $\eta_i \equiv 0$  almost everywhere. It can be reasoned from (5) that  $\forall i \leq k$ ,  $\lambda_i \equiv 0$ . The term “almost everywhere” means a proposition holds for all points except for a zero-measure set [41].

Furthermore, for the case where  $k = 1$ ,  $\lambda_1$  keeps continuous despite the junction condition (10). According to (9),

$$\mathcal{H}^\pm = \lambda_0 + \lambda_1^\pm u^\pm + \sum_{k=2}^n \lambda_k x_{k-1} = 0. \quad (11)$$

From  $\mathcal{H}^+ = \mathcal{H}^-$ ,  $\lambda_1^+ u^+ = \lambda_1^- u^-$ . The notation  $\bullet^\pm$  means the left and right-hand limits of variable  $\bullet$  at the junction time. Note that  $u^+ = 0$ ,  $u^- = M_0$ ,  $\lambda_1^+ = 0$ , so  $\lambda_1^- = 0$ . Therefore,  $\lambda_1^+ = \lambda_1^- = 0$ , i.e.,  $\lambda_1$  keeps continuous at the junction time.

It is noted that the case where  $|x_n| \equiv M_n$  for a period of time does not exist. By contradiction, if  $\exists t_1 < t_2$ , s.t.  $\forall t \in [t_1, t_2]$ ,  $|x_n(t)| \equiv M_n$ , then  $x_1(t) = x_2(t) = \dots = x_{n-1}(t) = 0$  during  $t \in [t_1, t_2]$ . In other words, the system state vector  $x$  parks at  $\pm M_n e_n$  for a period of time, which contradicts the time-optimality. As a corollary, (5) can be written as

$$\begin{cases} \dot{\lambda}_k = -\lambda_{k+1} - \eta_k \operatorname{sgn}(x_k), & k < n, \\ \dot{\lambda}_n = 0, \end{cases} \quad (12)$$

since  $\eta_n = 0$  almost everywhere. It should be pointed out that  $\lambda_n$  might not be constant though  $\dot{\lambda}_n = 0$ , because  $\lambda_n$  might jump when  $|x_n|$  touches  $M_n$  in the following Case 2.

An example of Case 1 is shown in Fig. 2.  $|x_1| \equiv M_1$  during  $t \in [t_1, t_2] \cup [t_5, t_6]$ , but  $\lambda_1$  keeps continuous despite to the junction condition (10).  $x_2 \equiv M_2$  during  $t \in [t_3, t_4]$ , and  $\lambda_2$  jumps decreasingly at  $t_3$  and  $t_4$ .

2) *Case 2.  $|x_k|$  Touches  $M_k$  at A Single Time Point:*

Without loss of generality, assume that  $x_k$  touches  $M_k$  at  $t_1$ , i.e.,  $x_k(t_1) = M_k$ , and  $\exists \delta > 0$ ,  $\forall t \in (t_1 - \delta, t_1) \cup (t_1, t_1 + \delta)$ ,  $x_k(t) < M_k$ . The case where  $x_k$  touches  $-M_k$  can be reasoned similarly.

The case where  $k = 1$  is evident to Case 1 in Section III-A1. Without loss of generality, assume  $x_1$  touches  $M_1$  at  $t_1$ .  $\exists \varepsilon > 0$ ,  $\forall t \in (0, \varepsilon)$ ,  $u(t_1 + t) < 0$ , while  $u(t_1 - t) > 0$ . By (8),  $\forall t \in (0, \varepsilon)$ ,  $\lambda_1(t_1 - t) \leq 0 \leq \lambda_1(t_1 + t)$ ; hence,  $\lambda_1(t_1^+) \geq \lambda_1(t_1^-)$ . (10) indicates that  $\lambda_1(t_1^+) - \lambda_1(t_1^-) \leq 0$ . So  $\lambda_1(t_1^+) = \lambda_1(t_1^-) = 0$ , i.e.,  $\lambda_1$  keeps continuous at  $t_1$ .

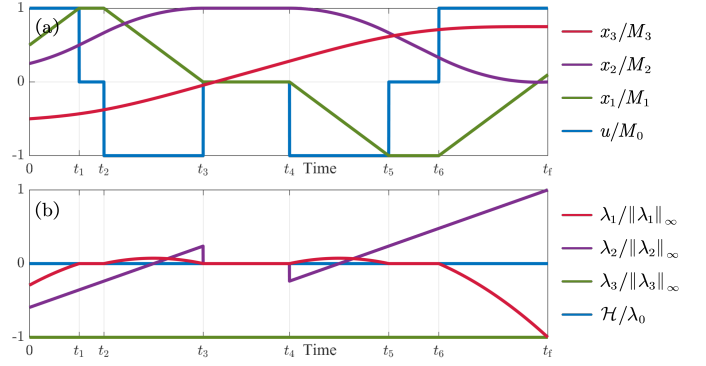


Fig. 2. A 3rd order optimal trajectory represented by  $\overline{0102010}$  in this paper, where  $\lambda_0 > 0$ . (a) The state vector. (b) The costate vector.

For the case where  $k \geq 2$ ,  $\exists \varepsilon \in (0, \delta)$ , s.t.  $\forall t \in (0, \varepsilon)$ ,  $u(t_1 + t) \equiv u^+$ , and  $u(t_1 - t) \equiv u^-$ . (a) If  $x_{k-1} = x_{k-2} = \dots = x_1 = 0$  at  $t_1$ , then  $\forall t \in (0, \varepsilon)$ ,  $x_k(t_1 + t) = M_k + \frac{u^+}{k!} t^k < M_k$ , and  $x_k(t_1 - t) = M_k + \frac{u^-}{k!} (-t)^k < M_k$ . Then,  $u^+ = -M_0$ ,  $u^- = (-1)^{k-1} M_0$ . (b) If  $\exists i = 1, 2, \dots, k-1$ ,  $x_i(t_1) \neq 0$ , then let  $h^* = \operatorname{argmin} \{h : x_{k-h}(t_1) \neq 0\} > 1$ , noting that  $x_{k-1}(t_1) = \frac{dx_k}{dt} \big|_{t=t_1} = 0$ . Since  $x_{k-h^*}$  is continuous,  $\exists \tilde{\varepsilon} \in (0, \varepsilon)$ ,  $\forall t \in (-\tilde{\varepsilon}, \tilde{\varepsilon})$ ,  $|x_{k-h^*}(t_1 + t) - x_{k-h^*}(t_1 - t)| < \frac{1}{2} |x_{k-h^*}(t_1)|$ ; hence,  $\operatorname{sgn}(x_{k-h^*}(t_1 + t)) \equiv \operatorname{sgn}(x_{k-h^*}(t_1))$ . By Taylor expansions of  $x_k$  at  $t_1$ ,  $\forall t \in [-\tilde{\varepsilon}, \tilde{\varepsilon}]$ ,  $\exists \theta_t \in (0, 1)$ ,  $x_k(t_1 + t) - x_k(t_1) = \frac{t^{h^*}}{h^{*1}} x_{k-h^*}(t_1 + \theta_t t) < 0$ . Therefore,  $x_{k-h^*}(t_1) < 0$  and  $h^*$  is even.

For cases where (a)  $n \leq 2$ , and where (b)  $n = 3$  with  $M_3 = \infty$ , there exist costate vectors for optimal trajectories which do not jump when Case 2 occurs, noting that the costate vector can be non-unique for one optimal solution. For the case where  $n = 3$  with  $M_3 < \infty$ , the jerk-limited time-optimal problem under position constraints is still not well solved yet. He et al. [11] developed the analytic expression of switching surfaces in 3rd order with zero terminal states, where Case 2, fortunately, does not exist with zero terminal states. Reflexxes [18] and Ruckig in community version [19], the two most famous open-source online trajectory planning packages, are not able to plan jerk-limited trajectories under position constraints.

An example of Case 2 is shown in Fig. 3. Though  $\dot{\lambda}_3 \equiv 0$  almost everywhere,  $\lambda_3$  jumps at  $t_3$  since  $x_3$  touches  $M_3$  at  $t_3$ . Two critical corollary based on analysis above are as follows:

**Proposition 1** (Bang-Singular-Bang Control Law). *The optimal control  $u(t)$  of (1) satisfies*

$$u(t) = \begin{cases} M_0, & \lambda_1(t) < 0 \\ 0, & \lambda_1(t) = 0 \\ -M_0, & \lambda_1(t) > 0 \end{cases} \quad (13)$$

almost everywhere.

*Proof.*  $\lambda_1(t) \equiv 0$  occurs only if  $\exists k$ , s.t.  $|x_k(t)| \equiv M_k$ , or else  $\lambda(t) \equiv 0$ . If  $\lambda(t) \equiv 0$ , then (9) implies that  $\lambda_0 = 0$ , which contradicts  $(\lambda_0, \lambda(t)) \neq 0$ . Therefore,  $u(t) \equiv 0$  if  $\lambda_1(t) \equiv 0$ . Hence, (13) is equivalent to (8) almost everywhere.  $\square$

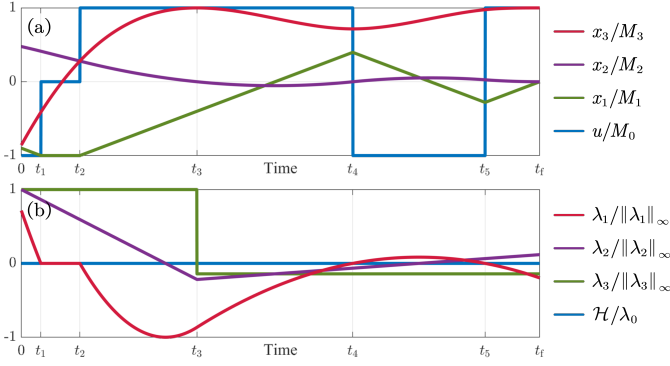


Fig. 3. A 3rd order optimal trajectory represented by  $01\bar{0}(\bar{3}, 2)\bar{0}0\bar{0}$  in this paper, where  $\lambda_0 > 0$ . (a) The state vector. (b) The costate vector.

**Proposition 2.** *If problem (1) is feasible, then (1) has a unique optimal control in an almost everywhere sense. In other words, if  $u = u_1^*(t)$  and  $u = u_2^*(t)$ ,  $t \in [0, t_f^*]$ , are both the optimal control of (1), then  $u_1^*(t) = u_2^*(t)$  almost everywhere.*

*Proof.* Denote  $\mu$  as the Lebesgue measure [41] on  $\mathbb{R}$ , and  $Q_1 \triangleq \{t : u_1^*(t), u_2^*(t) \in \{0, \pm M_0\}\}$ . From Proposition 1,  $\mu(Q_1) = t_f^*$ . Let  $Q_2 \triangleq \{t : u_1^*(t) \neq u_2^*(t)\}$ . If  $\mu(Q_2) > 0$ , then denote  $u_3^*(t) = \frac{1}{4}u_1^*(t) + \frac{3}{4}u_2^*(t)$ ,  $t \in [0, t_f^*]$ . It can be verified that  $u_3^*(t)$  is also an optimal control of problem (1). However,  $\forall t \in Q_1 \cap Q_2$ ,  $u_3^*(t) \notin \{0, \pm M_0\}$ ; hence,  $\mu\{u_3^*(t) \notin \{0, \pm M_0\}\} > \mu(Q_1 \cap Q_2) = \mu(Q_2) > 0$ , which contradicts Proposition 1. Therefore,  $\mu(Q_2) = 0$ .  $\square$

### B. System Behavior

The case where the inequality constraints (1d) hold strictly, i.e.,  $\forall k, |x_k| < M_k$ , is first considered. Bellman's principle of optimality [42] is necessary to introduce.

**Lemma 1** (Bellman's Principle of Optimality). *An optimal path has the property that whatever the initial conditions and control variables are, the remaining chosen control must be optimal for the remaining problem, with the state resulting from the early controls taken to be the initial condition.*

For problem (1), i.e.,  $\mathcal{P}(x_0, x_f; \mathbf{M})$ , Bellman's principle of optimality gives the results that if  $u = u^*(t)$  is the optimal control and  $\mathbf{x} = \mathbf{x}^*(t)$  is the optimal trajectory, then  $\forall [t_1, t_2] \subset [0, t_f]$ ,  $u^*|_{t \in [t_1, t_2]}$  is the optimal control of problem  $\mathcal{P}(\mathbf{x}^*(t_1), \mathbf{x}^*(t_2); \mathbf{M})$ .

For the case where  $\forall t \in [t_1, t_2]$ ,  $\forall k, |x_k(t)| < M_k$ , it is evident that  $\boldsymbol{\lambda}$  does not jump and  $\boldsymbol{\eta} \equiv \mathbf{0}$  in this period. Therefore,

$$\begin{cases} \dot{\lambda}_k = -\lambda_{k+1}, & k < n \\ \dot{\lambda}_n = 0 \end{cases}, \text{ if } \forall t \in [t_1, t_2], |\mathbf{x}(t)| < \mathbf{M}. \quad (14)$$

Since  $\boldsymbol{\lambda}$  is continuous, (14) indicates that  $\lambda_k(t)$  is an  $(n-k)$ -th degree polynomial for  $t \in [t_1, t_2]$ . According to the fundamental theorem of algebra [41],  $\lambda_k$  has no more than  $(n-k)$  roots during  $t \in [t_1, t_2]$ . A corollary, also well-known in previous works [13], is reasoned as follows:

**Proposition 3.** *Assume  $\forall t \in [t_1, t_2]$ ,  $\forall k, |x_k| < M_k$  in problem (1). Then, the optimal control  $u$  switches between  $M_0$  and  $-M_0$  with no more than  $(n-1)$  times.*

*Proof.* If  $\forall t \in [t_1, t_2]$ ,  $\forall k, |x_k| < M_k$ , then  $\boldsymbol{\lambda}$  is continuous. Specifically,  $\lambda_n \equiv \text{const}$ . By (14),  $\lambda_1$  is an  $(n-1)$ -th degree polynomial for  $t \in [t_1, t_2]$ . Note that  $\lambda_1 \equiv 0$  contradicts (9) when  $\boldsymbol{\eta} \equiv \mathbf{0}$ . Therefore,  $\lambda_1$  has no more than  $(n-1)$  roots. According to Proposition 1,  $u$  switches between  $M_0$  and  $-M_0$  with no more than  $(n-1)$  times.  $\square$

The properties of states and costates reasoned in Section III-A and Section III-B is summarized as follows:

**Theorem 1.** *The following propositions hold for the optimal control of problem (1).*

- 1)  $u(t) = -\text{sgn}(\lambda_1(t))M_0$  almost everywhere. Specifically,  $u(t) \equiv 0$  if  $\lambda_1(t) \equiv 0$ .
- 2)  $\forall t \in [0, t_f]$ ,  $\boldsymbol{\lambda}(t) \neq \mathbf{0}$ .
- 3)  $\lambda_1$  and  $\mathbf{x}$  are continuous, while  $\lambda_k$  ( $k > 1$ ) might jump at junction time.
- 4)  $\lambda_k$  consists of  $(n-k)$ -th degree polynomials and zero. Specifically,  $\lambda_1 \equiv 0$  for a period of time if and only if  $\exists k, |x_k| \equiv M_k$  during the period of time.
- 5) For  $k < n$ , cases might exist where  $\exists t_1 < t_2, \delta > 0$ , s.t.  $\forall t \in [t_1, t_2]$ ,  $|x_k(t)| \equiv M_k$ , while  $\forall t \in (t_1 - \delta, t_1) \cup (t_2, t_2 + \delta)$ ,  $|x_k(t)| < M_k$ . Then,  $\forall t \in [t_1, t_2]$ ,
  - a)  $\forall i \leq k$ ,  $\lambda_i(t) \equiv 0$ , while  $\forall i > k$ ,  $\lambda_i(t)$  is an  $(n-i)$ -th degree polynomial. Furthermore,  $\lambda_{k+1}(t)$  is not always zero.
  - b)  $u(t) \equiv 0, \forall i < k, x_i(t) \equiv 0$ .
  - c)  $\forall i \neq k$ ,  $\lambda_i$  is continuous. Only if  $1 < k < n$ ,  $\lambda_k$  might jump at  $t_1$  and  $t_2$ .
- 6) For  $k > 2$ , case might exist where  $\exists t_1 \in (0, t_f)$ ,  $\delta > 0$ , s.t.  $|x_k(t_1)| = M_k$ , while  $\forall t \in (t_1 - \delta, t_1) \cup (t_1, t_1 + \delta)$ ,  $|x_k(t)| < M_k$ . Then,  $\lambda_k$  might jump at  $t_1$ , and one and only one of the following cases holds:
  - a)  $\exists l < \frac{k}{2}$ , s.t.  $x_{k-1} = x_{k-2} = \dots = x_{k-2l+1} = 0$  at  $t_1$ , while  $x_{k-2l}(t_1) \neq 0$ , and  $\text{sgn}(x_{k-2l}(t_1)) = -\text{sgn}(x_k(t_1))$ . Denote  $h = 2l$  as the degree of  $|x_k(t_1)| = M_k$ .
  - b)  $x_{k-1} = x_{k-2} = \dots = x_1 = 0$  at  $t_1$ .  $u(t_1^+) = -\frac{M_0}{M_k}x_k(t_1)$ , and  $u(t_1^-) = (-1)^{k-1}\frac{M_0}{M_k}x_k(t_1)$ . Denote  $h = k$  as the degree of  $|x_k(t_1)| = M_k$ .

*Proof.* Based on discussion in Section III-A and Section III-B, Theorem 1 is evident.  $\square$

Theorem 1 fully lists system behaviors in a single stage of a sub-arc without limit points of chattering phenomena in an optimal trajectory, since connection between an unconstrained arc with positive length and constrained boundary has been fully discussed. The system behavior is classified into finite ones and is proposed formally as follows:

**Definition 1.** *System behavior* of problem (1) at a single stage is denoted as follows:

- 1) The stage where  $u \equiv M_0$  ( $-M_0$ ) is denoted as  $\bar{0}$  ( $\underline{0}$ ).
- 2) The stage where  $x_k \equiv M_k$  ( $-M_k$ ),  $u \equiv 0$ , and  $\forall i < k, x_i \equiv 0$ , is denoted as  $\bar{k}$  ( $\underline{k}$ ).



- 3)  $\forall 0 \leq k \leq n$ , the signs of  $\bar{k}$  and  $\underline{k}$  are denoted as  $\text{sgn}(\bar{k}) = 1$ ,  $\text{sgn}(\underline{k}) = -1$ . The value of  $\bar{k}$  and  $\underline{k}$  is denoted as  $|\bar{k}| = |\underline{k}| = k$ .

Based on Theorem 1 and Definition 1, system behaviors during the whole moving process can be studied. In the following, the sign of a system behavior can be left out if no ambiguity exists.

### C. Switching Law and Optimal-Trajectory Manifold

Building on the analysis of the system behavior in Section III-A and Section III-B, this section focuses on how the system behavior switches along the time-optimal trajectory. The core idea in this section is the switching law and the optimal-trajectory manifold for time-optimal control, which are defined in Section III-C1. The properties of the switching law on dimension and sign are reasoned in Section III-C2 and Section III-C3, respectively.

#### 1) Definitions:

**Definition 2.** Given a problem  $\mathcal{P}$ , assume the time-optimal trajectory passes through system behaviors  $s_1, s_2, \dots, s_N$  successively. Then, the series of system behaviors  $S = s_1 s_2 \dots s_N$  is called the **switching law** w.r.t.  $\mathcal{P}$ , denoted as  $S = S(\mathcal{P})$ , where  $N \in \mathbb{N}^*$  is called the length of  $S$ .

The switching law of a problem is unique according to Proposition 2. As an example, two second order optimal problems with the same terminal state vector are shown in Fig. 4. The switching law of  $\mathcal{P}_1 = \mathcal{P}(x_0^{(1)}, x_f; M)$  is  $S(\mathcal{P}_1) = 0\underline{1}\bar{0}$ . In other word, along the time-optimal trajectory from  $x_0^{(1)}$  to  $x_f$ ,  $\exists 0 < t_1 < t_2 < t_3 < t_f$ , s.t.

- 1)  $\underline{0}$ :  $\forall t \in (0, t_1)$ ,  $u(t) \equiv -M_0$ .  $x$  starts from  $x(0) = x_0^{(1)}$ , and  $x_1$  enters  $-M_1$  at  $t_1$ .
- 2)  $\underline{1}$ :  $\forall t \in (t_1, t_2)$ ,  $x_1(t) \equiv -M_1$ , while  $u(t) \equiv 0$ .
- 3)  $\bar{0}$ :  $\forall t \in (t_2, t_f)$ ,  $u(t) \equiv M_0$ .  $x_1$  exits  $-M_1$  at  $t_2$ , and the system state vector  $x$  reaches the terminal state vector  $x_f$  at  $t_f$ .

A similar analysis applies to  $\mathcal{P}_2 = \mathcal{P}(x_0^{(2)}, x_f; M)$ . From examples shown in Fig. 4, it can be observed that the switching law depends on the initial states.

Notably, a switching law focuses on how the system behavior switches along the trajectory, without information on motion time. The optimal control of problem (1) consists of a switching law and motion time for every system behavior, the definite condition of which will be discussed in Section III-D.

For an  $n$ -th order problem (1), a natural approach is to employ mathematical induction, utilizing the solutions of lower-order problems to solve the  $n$ -th order problem. The above idea induces the definitions of sub-problem and optimal-trajectory manifold.

For convenience of discussion, the optimal trajectory, the optimal control, and the terminal time of a problem  $\mathcal{P}$  are denoted as  $x^*(t; \mathcal{P})$ ,  $u^*(t; \mathcal{P})$ , and  $t_f^*(\mathcal{P})$ , respectively.

**Definition 3.** For an  $n$ -th order problem  $\mathcal{P} = \mathcal{P}(x_0, x_f; M)$  and  $0 \leq a_i \leq b_i \leq n$ ,  $a_1, a_2 \geq 1$ , a **sub-problem** of  $\mathcal{P}$  is  $\hat{\mathcal{P}} =$

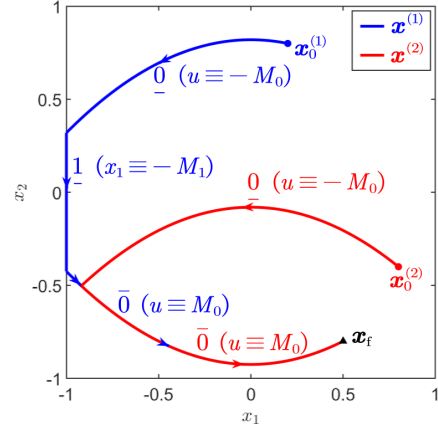


Fig. 4. Switching laws for 2 optimal problems with the same terminal state vector  $x_f$ , i.e.,  $\mathcal{P}_1 = \mathcal{P}(x_0^{(1)}, x_f; M)$  and  $\mathcal{P}_2 = \mathcal{P}(x_0^{(2)}, x_f; M)$ . Among them,  $n = 2$ ,  $M = (1, 1, 1)$ ,  $S(\mathcal{P}_1) = 0\underline{1}\bar{0}$ , and  $S(\mathcal{P}_2) = \underline{0}\bar{0}$ .

$\mathcal{P}(x_0^{a_1:b_1}, x_f^{a_2:b_2}; M^{a_3:b_3})$ , i.e., the time-optimal problem for chain-of-integrators with the following constraints:

$$\begin{cases} x_k(0) = x_{0k}, & a_1 \leq k \leq b_1 \\ x_k(t_f) = x_{fk}, & a_2 \leq k \leq b_2, \\ |x_k| \leq M_k, & a_3 \leq k \leq b_3. \end{cases} \quad (15)$$

**Definition 4.** Two time-optimal problems  $\mathcal{P}_1, \mathcal{P}_2$  are **equivalent**, denoted as  $\mathcal{P}_1 \Leftrightarrow \mathcal{P}_2$ , if  $\mathcal{P}_1$  and  $\mathcal{P}_2$  have the same solution of optimal control, i.e.,

$$\begin{cases} t_f^*(\mathcal{P}_1) = t_f^*(\mathcal{P}_2), \\ u^*(t, \mathcal{P}_1) = u^*(t, \mathcal{P}_2) \text{ almost everywhere.} \end{cases} \quad (16)$$

The equivalence between two problems is well-defined since the optimal for each problem is unique, according to Proposition 2. Two problems are equivalent when their boundary conditions can replace each other. Specifically, if a problem  $\mathcal{P}$  is equivalent to its sub-problem  $\hat{\mathcal{P}}$ , then some boundary conditions and constraints of  $\mathcal{P}$  is unnecessary. The above observation contributes to the following definition:

**Definition 5.** Given  $x_f \in \mathbb{R}^n$  and  $M \in \mathbb{R}_{++} \times \mathbb{R}_{++}^n$ , define

$$\mathcal{F}_k(x_f, M) \triangleq \bigcup \{x_0 \in \mathbb{R}^n : \mathcal{P}(x_0, x_f; M) \Leftrightarrow \mathcal{P}(x_0^{1:k}, x_f^{1:k}; M) \text{ are feasible}\} \quad (17)$$

as the  $k$ -th order **optimal-trajectory manifold** of  $x_f$  under  $M$ . Proposition 2 provides the well-posedness of  $\mathcal{F}_k(x_f, M)$ .

" $\Leftrightarrow$ " is evidently an equivalence relation among the set of feasible time-optimal control problems, which ensures the well-definedness of (17). Intuitively,  $\mathcal{F}_k(x_f, M)$  consists of time-optimal trajectories for  $k$ -th order sub-problem, with high-dimensional components of states additionally. The following proposition provides the nature of  $\mathcal{F}_k(x_f, M)$ .

**Proposition 4.** If  $\mathcal{F}_k = \mathcal{F}_k(x_f, M) \neq \emptyset$  in (17), then  $\mathcal{F}_k$  is an embedding of  $\mathbb{R}^k$  into  $\mathbb{R}^n$ , and  $\mathcal{F}_k$  is of dimension  $k$ .

*Proof.*  $\forall x_0, y_0 \in \mathcal{F}_k(x_f, M)$ ,  $\forall i \leq k$ ,  $x_{0i} = y_{0i}$ . According to the definition in (17),  $\mathcal{P}(x_0, x_f; M) \Leftrightarrow \mathcal{P}(y_0, x_f; M)$ ,



From Fig. 5(b), it is observed that  $\overline{2010}$  exists while  $\overline{2010}$  and  $\overline{2010}$  do not exist. The analysis of the sign is given as the following theorem.

**Theorem 3.**  $\forall S = s_1 s_2 \dots s_N \in \mathcal{SF}_k(x_f, M)$ ,  $\forall i = 2, 3, \dots, N$ ,

$$\text{sgn}(s_{i-1}) = \begin{cases} \text{sgn}(s_i), & \text{if } |s_i| \text{ is odd} \\ -\text{sgn}(s_i), & \text{if } |s_i| \text{ is even} \end{cases} \quad (24)$$

*Proof.* For the case where  $|s_{i-1}| = 0, |s_i| = 0$ , note that  $s_i \neq s_{i-1}$ . Hence,  $\text{sgn}(s_{i-1}) = -\text{sgn}(s_i)$ .

For the case where  $|s_{i-1}| \neq 0$ , according to Theorem 2,  $|s_i| = 0$ . Denote the switching time between  $s_{i-1}$  and  $s_i$  as  $T_i$ . If  $\text{sgn}(s_{i-1}) = +1$ , then  $\forall k < |s_{i-1}|$ ,  $x_k(T_i) = 0$  and  $x_{|s_{i-1}|}(T_i) = M_{|s_{i-1}|}$ . Assume that  $\text{sgn}(s_i) = +1$ , i.e.,  $u \equiv u_i = M_0$  during  $s_i$ . Then,  $\exists \delta > 0, \forall t \in (0, \delta)$ ,  $x_{|s_{i-1}|}(T_i + t) = M_{|s_{i-1}|} + \frac{1}{|s_{i-1}|!} M_0 t^{|s_{i-1}|} > M_{|s_{i-1}|}$  since  $u \equiv M_0$ , which leads to a contradiction. Therefore,  $\text{sgn}(s_{i-1}) = +1$  if  $\text{sgn}(s_i) = -1$ . For the similar analysis,  $\text{sgn}(s_{i-1}) = -1$  if  $\text{sgn}(s_i) = +1$ .

For the case where  $|s_i| \neq 0$ , according to Theorem 2,  $|s_{i-1}| = 0$ . Denote the switching time between  $s_{i-1}$  and  $s_i$  as  $T_i$ .  $x_k(T_i) = 0$  for  $k < |s_i|$  and  $x_{|s_i|}(T_i) = M_{|s_i|}$ . Then,  $\exists \delta > 0, \forall t \in (0, \delta)$ ,  $u(T_i - t) \equiv \text{sgn}(s_i) M_0$ ; hence,  $x_{|s_i|}(T_i - t) = \text{sgn}(s_i) M_{|s_i|} + \frac{1}{|s_i|!} M_0 t^{|s_i|} \cdot (-1)^{|s_i|} \text{sgn}(s_{i-1})$ . The constraint where  $|x_{|s_i|}(T_i - t)| \leq M_{|s_i|}$  resulting that  $(-1)^{|s_i|} \text{sgn}(s_{i-1}) = -\text{sgn}(s_i)$ .  $\square$

Theorem 3 indicates that signs of all system behaviors in a switching law is uniquely determined by the sign of the last system behavior. For a switching law  $S$  with a length of  $N$ , Theorem 3 reduces the possible signs of all system behaviors from  $2^N$  to 2.

#### D. Augmented Switching Law and Tangent Marker

For a given initial state vector  $x_0 \in \mathbb{R}^n$  and the switching law  $S = S(\mathcal{P}(x_0, x_f; M))$ , Section III-C2 has pointed out that the optimal control can be solved only if  $\dim S = n$ . For example, in Fig. 5(a),  $x_0 \in \mathbb{R}^2$  is given. If  $S = \overline{00}$ , then the full definite conditions are provided by (20), (21), and (22). However,  $S = \overline{000}$  is underdefined, while  $S = \overline{0}$  is overdefined; hence, the optimal control can be solved directly from neither  $S = \overline{000}$  nor  $S = \overline{0}$  by (20), (21), and (22). The augmented switching law should be proposed to solve the problem.

**Definition 7.** Given a problem  $\mathcal{P}$ , an **augmented switching law** w.r.t.  $\mathcal{P}$ , denoted as  $S \in \mathcal{AS}(\mathcal{P})$ , is the switching law of  $\mathcal{P}$  attached full definite conditions.

Definite conditions attached on an augmented switching law  $S$  should guarantee that  $\dim S = n$  for an  $n$ -th order problem. In the above example where  $n = 2$ ,  $\dim \overline{00} = 2$ ,  $\dim \overline{000} = 3 > 2$ , and  $\dim \overline{0} < 2$ . Therefore,  $\overline{00}$  provides full definite conditions and is an augmented switching law, while  $\overline{000}$  and  $\overline{0}$  are not. As a trick, the switching law  $\overline{0}$  can be represented by an augmented switching law  $\overline{00}$  or  $\overline{00}$ , where the motion time of  $\overline{0}$  is 0. This example also shows that the augmented switching law of a problem can be not unique.

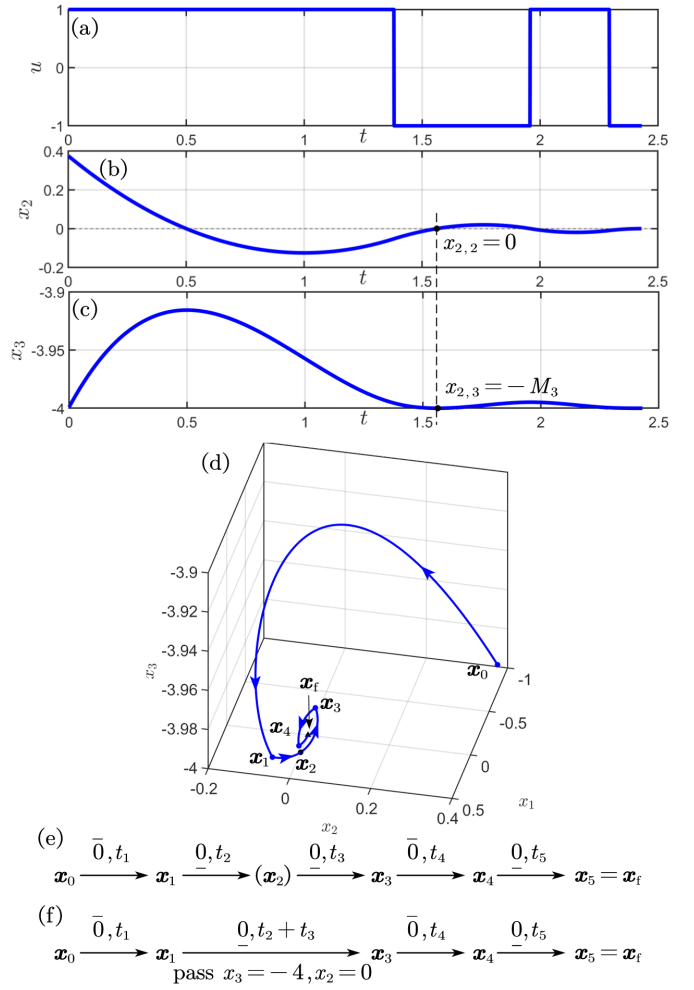


Fig. 6. Time-optimal trajectory with a tangent marker.  $\mathcal{P} = \mathcal{P}(x_0, x_f; M)$ , where  $M = (1, 1, 1.5, 4)$ . An augmented switching law for  $\mathcal{P}$  is  $S' = \overline{00}(3, 2)\overline{000} \in \mathcal{AS}(\mathcal{P})$ , where the tangent marker  $(3, 2)$  means  $x_{2,3} = -4, x_{2,2} = 0$ , and  $x_{2,1} > 0$ . (a), (b) and (c) are the jerk, velocity, and position plots, respectively. (d) is the trajectories of system states  $x$ . (e) and (f) are the flow charts for  $S' \in \mathcal{AS}(\mathcal{P})$  and  $S = S(\mathcal{P})\overline{0000}$ .

However, the above trick of adding zero is not enough to provide all augmented switching laws. According to discussion on Case 2 in Section III-A2, the tangent marker is necessary to define as a kind of definite condition and precisely exists in the time-optimal problem (1).

**Definition 8.** For a time-optimal trajectory, assume  $|x_k|$  touches  $M_k$  at  $t_1$  with a degree  $h = k$  or an even degree  $h < k$ , as described in Theorem 1-6. Then, the **tangent marker** is denoted as  $(s, h)$ , where  $|s| = k$  and  $\text{sgn}(s) = \text{sgn}(x_k(t_1))$ .

**Theorem 4.**  $S = S_1(s, h)S_2$ , where  $S_i = s_1^{(i)}s_2^{(i)} \dots s_{N_i}^{(i)}$  are augmented switching laws,  $i = 1, 2$ , then,

- 1)  $|s_{N_1}^{(1)}| = |s_1^{(2)}| = 0$ .
- 2)  $(s, h)$  contributes  $-h < 0$  dimension.

*Proof.* According to Section III-A2,  $|s_{N_1}^{(1)}| = |s_1^{(2)}| = 0$ , and  $(s, h)$  does not provide extra motion time. Assume the state vector at  $(s, h)$  is  $x_1$ . Then,  $(s, h)$  contributes  $h$  extra constraints, i.e.,  $x_{1,|s|} = \text{sgn}(s)M_{|s|}$ , and  $x_{1,|s|-k} = 0, k =$



$1, 2, \dots, h-1$ . Hence,  $(s, h)$  contributes  $-h$  dimension.  $\square$

Fig. 6 shows an example of the tangent marker. From Fig. 6(a), it is observed that  $\mathcal{S}(\mathcal{P}) = \underline{0000}$ . Therefore,  $\dim \mathcal{S}(\mathcal{P}) = 4 > 3$ . Hence, the problem  $\mathcal{P}$  is not determined by  $\mathcal{S}(\mathcal{P})$ . Opportunely,  $S' = \underline{00}(\underline{3}, 2)\underline{000} \in \mathcal{AS}(\mathcal{P})$ , where the tangent marker  $(\underline{3}, 2)$  induced 2 constraints, i.e.,  $x_{2,3} = -M_2$  and  $x_{2,2} = 0$ . Therefore,  $\dim S' = 5 - 2 = 3$ , and  $\mathcal{P}$  is determined by  $S'$ . As shown in Fig. 6(f),  $\underline{0}(\underline{3}, 2)\underline{0}$  with time  $t_2, t_3$  performs the same as  $\underline{0}$  with time  $t_2 + t_3$  on the surface, and  $(\underline{3}, 2)$  means the system state vector passes  $x_3 = -4$ ,  $x_2 = 0$  during the stage  $\underline{0}$ .

The physical meaning of the tangent marker  $(\underline{3}, 2)$  is clear. Without consideration of the constraint  $x_3 \geq -M_3$ , the switching law should be  $\underline{000}$ , where  $x_3 < -M_3$  occurs. To guarantee  $x_3 \geq -M_3$ , an accelerating stage  $\underline{0}$  is introduced first, then  $\underline{000}$  is applied for minimum motion time. The tangent marker  $(\underline{3}, 2)$  shows that the first stage  $\underline{0}$  lasts as short as possible. In other words, once the constraint  $x_3 \geq -M_3$  holds in the future, an optimal switching law  $\underline{000}$  is applied. Therefore, the constraint  $x_3 \geq -M_3$  is active, and  $(\underline{3}, 2)$  reflects some conditions for extremum.

Considering the full discussion in Section III-A, a conjecture is proposed that system behaviors and tangent markers can provide full definite condition for time-optimal trajectories.

**Conjecture 1.**  $\forall S$  is an augmented switching law of the time-optimal problem (1) where chattering phenomena do not occur,  $S$  consists of system behaviors in Definition 1 and tangent markers in Definition 8.

Obviously, if Conjecture 1 can be proven constructively, then there is a prospect of the time-optimal problem for high-order chain-of-integrator systems which is an open problem in the optimal control theory.

#### IV. MANIFOLD-INTERCEPT METHOD

Section III studies the properties of time-optimal control and builds a novel notation system of the time-optimal problem for chain-of-integrators. However, it is a daunting task to solve the optimal control for arbitrary given problems  $\mathcal{P}(x_0, x_f; M)$ , especially when a chattering phenomenon occurs. Based on conclusions of optimal control reasoned in Section III, this section proposed a trajectory planning method for high-order chain-of-integrators systems, named the manifold-intercept method (MIM).

It should be pointed out that MIM is an efficient and quasi-optimal method. As will be pointed out in Part II [37], chattering phenomena exist in 4th order or higher-order problem, which impedes the computation of optimal control. Section V will indicate that MIM is near-optimal for 4th or higher-order problems, and is able to avoid chattering. Furthermore, for 3rd or lower-order problems, MIM achieves time-optimality. In this section, the switching law and the optimal-trajectory manifold are corresponding to those induced by MIM. Propositions in Section III except Conjecture 1 still hold true, while theorems in this section might not be true for time-optimal control unless emphasized.

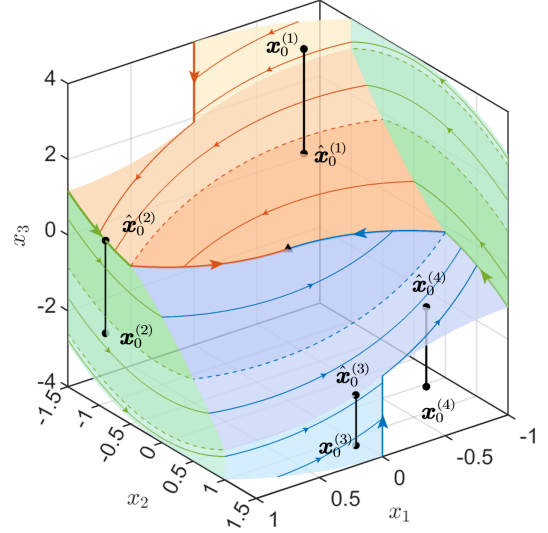


Fig. 7. Some examples of proper positions. The parameters and optimal-trajectory manifold is the same as Fig. 5(b).  $\forall i = 1, 2, 3, 4$ ,  $\hat{x}_0^{(i)}$  has a proper position and the same  $x_1, x_2, x_3$  as that of  $x_0^{(i)}$ .

##### A. Manifold-Intercept Method

The key idea of MIM is to follow a greedy-and-conservative principle. When the current state vector is “higher” (or “lower”) than the lower-order optimal-trajectory manifold of the terminal state vector, the control greedily chooses the minimum (or maximum) value to drive the system entering the constant velocity phase of minimum (or maximum) velocity, i.e.,  $n-1$  (or  $\overline{n-1}$ ) as quick as possible, conservatively considering state constraints. Once the states enters the lower order optimal-trajectory manifold, the states move along lower order trajectories to reach the terminal states, applying the Bellman’s principle of optimality in Lemma 1.

**Definition 9.** The **proper-position function** is defined as  $p^* : \text{dom } p^* \rightarrow \mathbb{R}$ ,  $(x_0, x_f; M) \mapsto \hat{x}_n$ , where

$$\text{dom } p^* = \{(x_0; x_f, M) : \mathcal{P}(x_0, x_f; M) \text{ is feasible}, \\ x_0, x_f \in \mathbb{R}^n, M \in \mathbb{R}_{++} \times \overline{\mathbb{R}}_{++}^n\}, \quad (25)$$

$$\text{s.t. } \hat{x}_0 \triangleq (x_{0,1}, x_{0,2}, \dots, x_{0,n-1}, \hat{x}_n) \in \mathcal{F}_{n-1}(x_f, M).$$

**Definition 10.** For a feasible problem  $\mathcal{P}(x_0, x_f; M)$  of  $n$ -th order,  $x_0$  is called **higher** (or **lower**) than  $\mathcal{F}_{n-1}(x_f, M)$ , if  $x_{0,n} >$  (or  $<$ )  $p^*(x_0; x_f, M)$ . If  $x_{0,n} = p^*(x_0; x_f, M)$ , then  $x_0$  is called to **have a proper position**.

The proper-position function is well-defined according to the proof process of Proposition 4. In Definition 9,  $\hat{x}_0$  can be regarded as the projection of  $x_0$  along the  $x_n$ -axis onto the manifold  $\mathcal{F}_{n-1}(x_f, M)$ . In Definition 10, the relationship between  $x_0$  and  $\mathcal{F}_{n-1}(x_f, M)$  is represented by the positional relationship between  $x_0$  and its projection, i.e.,  $\hat{x}_0$ .

A third order example is shown in Fig. 7.  $x_0^{(1)}$  is higher than  $\mathcal{F}_2(x_f, M)$ , while  $x_0^{(2)}$ ,  $x_0^{(3)}$ , and  $x_0^{(4)}$  are lower than  $\mathcal{F}_2(x_f, M)$ . In Fig. 7,  $\forall i = 1, 2, 3, 4$ ,  $\hat{x}_0^{(i)} \in \mathcal{F}_2(x_f, M)$  has a proper position.

Now MIM is introduced by mathematical induction.

For the base case, i.e.,  $n = 1$ , the optimal control has a trivial analytic expression, i.e.,

$$u^*(t) = M_0 \operatorname{sgn}(x_f - x_0), \forall 0 \leq t \leq t_f = \frac{|x_f - x_0|}{M_0}. \quad (26)$$

Assume that  $\forall 1 \leq k < n$ , the  $k$ -th order trajectories with arbitrary  $x_0, x_f, M$  can be planned by MIM. For the case where  $n \geq 2$  and  $M_n = \infty$ ,  $\hat{x}_n = p^*(x_0; x_f, M)$  can be calculated by solving  $\mathcal{P}(x_0^{1:(n-1)}, x_f^{1:(n-1)}; M^{0:(n-1)})$ . By Definition 9, it can be judged whether  $x_0$  is higher or lower than  $\mathcal{F}_{n-1}(x_f, M)$  by comparing  $x_{0,n}$  and  $\hat{x}_n$ .

- 1) If  $x_0$  has a proper position, according to (17),  $\mathcal{P} \triangleq \mathcal{P}(x_0, x_f; M)$  has the same solution as the  $(n-1)$ -th order problem  $\mathcal{P}(x_0^{1:(n-1)}, x_f^{1:(n-1)}; M^{0:(n-1)})$ .
- 2) If  $x_0$  is higher than  $\mathcal{F}_{n-1}(x_f, M)$ , the system tends to obtain a state vector in minimum uniform speed  $-M_{n-1}$ , and keeps the velocity as  $-M_{n-1}$  until entering  $\mathcal{F}_{n-1}(x_f, M)$ .

- a) Firstly, the system state vector moves along the MIM-trajectory of the  $(n-1)$ -th order problem  $\mathcal{P}_1 = \mathcal{P}(x_0^{1:(n-1)}, -M_{n-1}e_{n-1}; M^{0:(n-1)})$ , i.e.,  $x(t) = x^*(t; \mathcal{P}_1)$ .
- b) If  $x(t_f^*(\mathcal{P}_1))$  is still higher than  $\mathcal{F}_{n-1}(x_f, M)$ , denote  $\hat{x}_n = p^*(-M_{n-1}e_{n-1}; x_f, M)$ . Then,  $u(t) \equiv 0$  for  $t \in [t_f^*(\mathcal{P}_1), t_1 + t_f^*(\mathcal{P}_1)]$ , where  $t_1 = \frac{x_n(t_f^*(\mathcal{P}_1)) - \hat{x}_n}{M_{n-1}}$ . Therefore,  $x(t_1) = -M_{n-1}e_{n-1} + \hat{x}_n e_n$  has a proper position. Denote  $\mathcal{P}_2 = \mathcal{P}(-M_{n-1}e_{n-1}, x_f^{1:(n-1)}; M^{0:(n-1)})$ . Let  $x$  moves along the MIM-trajectory of  $\mathcal{P}_2$ , i.e.,  $x(t_f^*(\mathcal{P}_1) + t_1 + t) = x^*(t; \mathcal{P}_2)$ ,  $0 \leq t \leq t_f^*(\mathcal{P}_2)$ . Finally,  $x(t_f^*(\mathcal{P}))$  reach  $x_f$ , i.e.,

$$t_f^*(\mathcal{P}) = t_f^*(\mathcal{P}_1) + t_1 + t_f^*(\mathcal{P}_2). \quad (27)$$

- c) If  $x(t_f^*(\mathcal{P}_1))$  is lower than  $\mathcal{F}_{n-1}(x_f, M)$ , i.e.,  $x(t)$  enters  $\mathcal{F}_{n-1}(x_f, M)$  at some time  $t_2 \in (0, t_f^*(\mathcal{P}_1))$ , then  $x$  can move along the MIM-trajectory of the  $(n-1)$ -th order problem  $\mathcal{P}_3 = \mathcal{P}(x^{1:(n-1)}(t_2), x_f^{1:(n-1)}; M^{0:(n-1)})$ . Finally,  $x(t_f^*(\mathcal{P}))$  reach  $x_f$ , i.e.,

$$t_f^*(\mathcal{P}) = t_2 + t_f^*(\mathcal{P}_3). \quad (28)$$

- 3) If  $x_0$  is lower than  $\mathcal{F}_{n-1}(x_f, M)$ , a similar analysis as above applies to this case.

If  $M_{n-1} = \infty$  above, then the first terminal state vector in Case 2 is modified as  $-M_k e_k$  where  $k < n-1$  is maximum index satisfying  $M_k \neq \infty$ . Specifically, if  $k = 0$ , the problem degenerates into a time-optimal problem without state constraints, which can be easily solved by an  $n$ -th order polynomial system [14].

An example of Case 2b is  $x^{(1)}$  in Fig. 4, where  $x^{(1)}$  slides under a minimum velocity  $-M_1$  uniformly until  $x$  enters  $\mathcal{F}_1(x_f, M)$ . An example of Case 2c is  $x^{(2)}$  in Fig. 4, where  $x^{(2)}$  is intercepted by  $\mathcal{F}_1(x_f, M)$  before  $x^{(2)}$  reaches  $x_1 = -M_1$ .

The above  $n$ -th order process meets the Bang-Singular-Bang control law and can be solved by sequential  $(n-1)$ -th order problems. Furthermore, the trajectory  $x(t) = x^*(t, \mathcal{P})$  meets the constraints  $\forall k = 1, 2, \dots, n$ ,  $|x_k| \leq M_k$ . Specifically,  $|x_n| \leq M_n = \infty$ .

For the case where  $n \geq 2$  and  $M_n < \infty$ , the optimal trajectory  $x(t) = x^*(t; \mathcal{P}_\infty)$  is generated based on the above process, where  $\mathcal{P}_\infty = \mathcal{P}(x_0, x_f; M^{0:(n-1)})$ .

- 1) If the trajectory  $x(t) = x^*(t; \mathcal{P}_\infty)$  meets the constraint  $|x_n| \leq M_n$ , then the constraint  $|x_n| \leq M_n$  is deactivated. Hence,  $x(t) = x^*(t; \mathcal{P}_\infty)$  is also the optimal trajectory of  $\mathcal{P} = \mathcal{P}(x_0, x_f; M)$ .
- 2) If the trajectory  $x(t) = x^*(t; \mathcal{P}_\infty)$  does not meet the constraint, i.e.,  $|x_n| > M_n$  at some time, then a tangent marker w.r.t.  $x_n$  occurs in the optimal problem  $\mathcal{P}$ . Considering the dimension of the augmented switching law and according to Theorem 1,  $\exists h \leq n$ , s.t.  $x$  reaches a tangent marker  $(n, h)$  through an augmented switching law of  $h$  dimension in optimal time, i.e., by solving an  $h$ -th order problem. Assume the system state vector is  $\hat{x}$  when reaching the tangent marker. Then, the system state vector can move from  $\hat{x}$  to  $x_f$  in optimal time by solving  $\mathcal{P}(\hat{x}, x_f; M^{0:(n-1)})$ .

By mathematical induction,  $\forall n \in \mathbb{N}^*$ , trajectories for high-order chain-of-integrators systems with full state constraints  $M \in \mathbb{R}_{++} \times \mathbb{R}_{++}^n$  and arbitrary terminal state vector  $x_f \in \mathbb{R}^n$  can be planned by MIM.

## B. Virtual System Behavior

The augmented switching law in this section refers to the switching law in MIM with full definite conditions. The virtual system behavior is defined for the case where (28) occurs.

**Definition 11.** In MIM, assume an augmented switching law is  $S = S_1 s(S_2) S_3 \in \mathcal{AS}(\mathcal{P}(x_0, x_f; M))$ , where  $s$  is a system behavior, and  $S_i = s_1^{(i)} s_2^{(i)} \dots s_{N_i}^{(i)}$ ,  $i = 1, 2, 3$  are augmented switching laws.  $(S_2)$  is called a **virtual system behavior**, if  $\exists t^{(i)} = \left(t_j^{(i)}\right)_{j=1}^{N_i} \geq 0, i = 1, 2, 3$  and  $t_1, t_2 \geq 0$ , s.t.

- 1)  $x_0$  moves to  $x_f$  successively passing through  $S_1$  by time  $t^{(1)}$ ,  $s$  by time  $t_1$ , and  $S_3$  by time  $t^{(3)}$ . In order words,  $S_1 s S_3$  with time  $(t^{(1)}, t_1, t^{(3)})$  is the solution of  $\mathcal{P}$ .
- 2)  $x_0$  can move successively passing through  $S_1$  by time  $t^{(1)}$ ,  $s$  by time  $t_2$ , and  $S_2$  by time  $t^{(2)}$ . In order words,  $S_1 s S_2$  with time  $(t^{(1)}, t_2, t^{(2)})$  is a feasible solution under constraints (21) and (22).

An example is shown in Fig. 8, where  $\mathcal{S}(\mathcal{P}) = 01\bar{0}2\bar{0}1\bar{0}01\bar{0}2\bar{0}1\bar{0}$  in MIM; hence,  $\dim \mathcal{S}(\mathcal{P}) = 6 > 4$ .  $S = 01\bar{0}2\bar{0}1\bar{0}(3)01\bar{0}2\bar{0}1\bar{0} \in \mathcal{AS}(\mathcal{P})$ ; hence,  $\dim S = 4$ . As shown in Fig. 8(d),  $x_{i-1}$  moves to  $x_i$  under the corresponding system state vector for time  $t_i$ ,  $i \neq 8, 9$ , while  $x_7$  moves to  $x_9$  under  $\bar{0}$  for time  $t_9$ . Furthermore, the ability of  $x_7$  that can moves to  $x_8$  under  $\bar{0}$  for a time period  $t_9$  provides definite condition for  $\mathcal{P}_2$ , where  $x_8$  is determined by the virtual system behavior (3), i.e.,  $x_{8,1} = x_{8,2} = 0$ ,  $x_{8,3} = -M_3 = -4$ .  $x$  is intercepted by  $\mathcal{F}_3(x_f, M)$  at  $x_7$ .

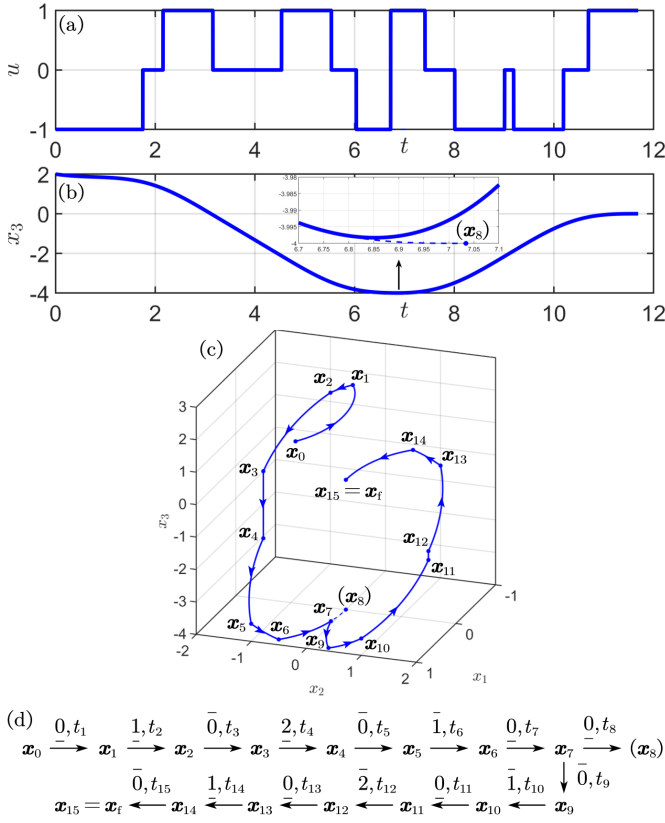


Fig. 8. An example of the virtual system behavior.  $M = (1, 1, 1.5, 4, 20)$ .  $S = 0102010(3)0102010 \in \mathcal{AS}(\mathcal{P})$ , where (3) is a virtual system behavior. (a) and (b) are the snap and velocity plots. (c) is the trajectory of the first three components of system states  $x^{1:3}$ . (d) is the flow charts for  $S$ .

**Theorem 5.** In MIM, apply notations in Definition 11.

- 1) The dimension of  $S$  can be calculated like (19), i.e.,  $(S_2)$  contributes  $\sum_{i=1}^{N_2} (1 - |s_i^{(2)}|) < 0$  dimension to  $S$ .
- 2)  $|s_1^{(3)}| = 0$ , and  $\text{sgn}(s) = -\text{sgn}(s_1^{(3)})$ .
- 3)  $|s_{N_2}^{(2)}| \neq 0$ , and  $\forall k < N_2$ ,  $|s_{N_2}^{(2)}| > |s_k^{(2)}|$ . Furthermore,  $\text{sgn}(s_{N_2}^{(2)}) = -\text{sgn}(s_1^{(3)})$ .
- 4) Except the tangent marker,  $S_2$  has an even number of even numbers, and (24) holds.
- 5) If  $\exists N'_2 < N_2$ , s.t.  $\dim S_{2, (N'_2+1):N_2} = 0$ , then  $(S_2)$  is equivalent to  $(S_{2, 1:N'_2})$ , i.e.,  $S$  is equivalent to  $S_1 s (S_{2, 1:N'_2}) S_3$ .

*Proof.* Theorem 5-1 holds by the same analysis as Theorem 2. Theorem 5-5 holds evidently.

Denote  $\mathcal{P} = \mathcal{P}(x_0, x_f; M)$ . According to Section IV-A, the virtual system behavior  $(S_2)$  occurs when the optimal trajectory represented by  $S_1 s S_2$  is intercepted by a low-dimensional optimal-trajectory manifold  $\mathcal{F}$ , and  $x$  moves in  $\mathcal{F}$  along an optimal trajectory represented by  $S_3$  after that. By induction, we only need to prove Theorem 5 for the case where the terminal state vector of  $S_1 s S_2$  has a maximum velocity, i.e.,  $|s_{N_2}^{(2)}| = n - 1$  for an  $n$ -th order problem.

According to discussion above,  $S_3 \in \mathcal{AF}_{n-1}$ ; hence,  $|s_1^{(3)}| = 0$ . Note that  $S_1 s S_3$  induces  $\mathcal{S}(\mathcal{P})$  by removing all

brackets, and  $s$  as well as  $s_1^{(3)}$  are system behaviors. According to Theorem 3,  $\text{sgn}(s) = -\text{sgn}(s_1^{(3)})$ . Theorem 5-2 holds.

Note that  $S_1 s S_2^{1:(N_2-1)}$  is an augmented switching law with the terminal states  $\pm M_{n-1} e_{n-1}$ . Therefore,  $|s_{N_2}^{(2)}| = n - 1 \neq 0$ , and  $|s_{N_2}^{(2)}| > |s_k^{(2)}|, \forall k < N_2$ . Furthermore,  $|s_1^{(1)}| = |s_{N_3}^{(3)}| = 0$  and  $\text{sgn}(s_{N_3}^{(3)}) = (-1)^{n-1} \text{sgn}(s_1^{(1)})$ . Note that  $S_3 \in \mathcal{AF}_{n-1}$ ; hence,  $\text{sgn}(s_{N_3}^{(3)}) = (-1)^{n-2} \text{sgn}(s_1^{(3)})$ . Assume  $x_0$  is higher than  $\mathcal{F}_{n-1}(x_f, M)$ . Then,  $\text{sgn}(s_{N_2}^{(2)}) = \text{sgn}(s_1^{(1)}) = -1$ ; hence,  $\text{sgn}(s_{N_2}^{(2)}) = -\text{sgn}(s_{N_3}^{(3)})$ . If  $x_0$  is lower than  $\mathcal{F}_{n-1}(x_f, M)$ , then  $\text{sgn}(s_{N_2}^{(2)}) = -\text{sgn}(s_{N_3}^{(3)}) = 1$ . Therefore, Theorem 5-3 holds.

According to discussion above, (24) holds for  $S_1 s S_2$ ,  $S_1 s S_3$ , and  $s_{N_2}^{(2)} S_3$ . In other words, the sign of  $S_1 s (S_2) S_3$  is the same as  $S_1 s S_2 S_3$  and satisfies (24). Note that  $\text{sgn}(s) = -\text{sgn}(s_1^{(3)}) = \text{sgn}(s_{N_2}^{(2)})$ ; hence,  $S_2$  has an even number of even numbers. Therefore, Theorem 5-4 holds.  $\square$

As an example for Theorem 5-5,  $0102(0103)0102010$  is equivalent to  $01020102010$ . The tangent marker also has some properties in MIM.

**Theorem 6.** Apply notations in Theorem 4. In MIM,

- 1)  $\text{sgn}(s_{N_1}^{(1)}) = \text{sgn}(s_1^{(2)}) = \text{sgn}(s)$ .
- 2)  $h < |s|$ . Moreover,  $h$  is even.

*Proof.* Similar to the proof of Theorem 5, we only need to prove the case where  $|s| = n$  for an  $n$ -th problem. Assume  $x_0$  is higher than  $\mathcal{F}_{n-1}(x_f, M)$  and the tangent marker occurs. According to Theorem 6,  $|s_{N_1}^{(1)}| = |s_1^{(2)}| = 0$ . According to Section IV-A,  $\text{sgn}(s_1) = (-1)^{d-2} \text{sgn}(s_1^{(1)}) = -1$ , and  $\text{sgn}(s) = -1$ . When  $x$  reaches  $(s, d)$  as  $\tilde{x}$ ,  $\tilde{x}$  is still higher than  $\mathcal{F}_{n-1}(x_f, M)$ , while  $s_2 S_2$  is the augmented switching law from  $\tilde{x}$  to  $x_f$ . Therefore,  $|s_2| = 0$ ,  $\text{sgn}(s_1) = -1$ . Applying a similar analysis to the case where  $x_0$  is lower than  $\mathcal{F}_{n-1}(x_f, M)$ , Theorem 6-1 holds.

Assume  $h = |s|$  and the system state vector reaches  $(s, h)$  at  $t$ . Then,  $u$  is continuous at  $t$  and  $u(t) = \text{sgn}(s) M_0$  by Theorem 6-1. However, according to Section III-A2,  $\text{sgn}(u(t)) = -\text{sgn}(s)$  since  $|x_{|s|}| \leq M_{|s|}$ , which causes contradiction. Therefore,  $h < |s|$ ; hence,  $h$  is even.  $\square$

Theorems 5 and 6 indicate that signs of elements of an augmented switching law with a length of  $N$  is determined by the sign of the last element in MIM, which also reduces the possible signs of all elements from  $2^N$  to 2. Furthermore, augmented switching laws can be enumerated fully, as reasoned in Section IV-C.

### C. Full Enumeration of Augmented Switching Laws in MIM

**Definition 12.** In MIM, assume  $\mathcal{F}_k(x_f, M) \neq \emptyset$  in (17). The augmented-switching-law representation of  $\mathcal{F}_k(x_f, M)$  is

$$\mathcal{AF}_k(x_f, M) = \bigcup \{S \in \mathcal{AS}(\mathcal{P}(x_0, x_f; M)) : x_0 \in \mathcal{F}_k(x_f, M), \dim S = k\}. \quad (29)$$

$\forall x_0 \in \mathcal{F}_k(x_f, M), \mathcal{P} = \mathcal{P}(x_0, x_f; M), S \in \mathcal{AS}(\mathcal{P})$ , if  $\dim S = k' < k$ ,  $(k - k')$  zero can be added before  $S$  to increase the dimension to  $k$ . For example, if  $S = \bar{0}\bar{0}$  in Fig. 5(b), the switching law can be seen as  $\bar{0}\bar{0}\bar{0}$ , and the solved motion time of the first  $\bar{0}$  is 0. If some augmented switching laws do not end with 0, then some 0 can also be added after the augmented switching law with motion time 0.

**Definition 13.** In MIM,

$$\mathcal{AF}_n \triangleq \bigcup_{\substack{x_f \in \mathbb{R}^n \\ M \in \mathbb{R}_{++} \times \mathbb{R}_{++}^n}} \mathcal{AF}_n(x_f, M) \quad (30)$$

is called the  $n$ -th order set of augmented switching laws.

According to analysis in Section IV-A,  $\mathcal{AF}_n$  can be constructed as follows:

**Theorem 7.** In MIM,  $\mathcal{AF}_1 = \{0\}$ .  $\forall n \geq 1, \mathcal{AF}_{n+1} \supset F_{n,1} \cup F_{n,2} \cup F_{n,3}$ , where

$$F_{n,1} = \{S_1 S_2 : S_1, S_2 \in \mathcal{AF}_n, |s| = n\}, \quad (31)$$

$$F_{n,2} = \{S_1 (S_2 s) S_3 : S_1 S_2, S_3 \in \mathcal{AF}_n, |s| = n, \\ S_2 s \text{ satisfies Theorem 5-4}\}, \quad (32)$$

$$F_{n,3} = \{S_1 (s, d) S_2 : S_1 \in \mathcal{AF}_d, S_2 \in F_{n,1} \cup F_{n,2}, \\ |s| = n + 1, d < |s| \text{ is even}\}. \quad (33)$$

The signs of system behaviors, tangent markers, and virtual system behaviors satisfy Theorems 3, 4, 5, and 6.

*Proof.* According to Theorems 5, 6, and discussion in Section IV-A, Theorem 7 holds evidently.  $\square$

For example,  $\mathcal{AF}_2 = \{00, 010\}$ .  $\mathcal{AF}_3 = \{000, 0010, 0100, 01010, 00200, 002010, 010200, 0102010, 00(3,2)000, 00(3,2)0010, 00(3,2)0100, 00(3,2)01010, 00(3,2)00200, 00(3,2)002010, 00(3,2)010200, 00(3,2)0102010, 010(3,2)000, 010(3,2)0010, 010(3,2)0100, 010(3,2)01010, 010(3,2)00200, 010(3,2)002010, 010(3,2)010200, 010(3,2)0102010\}$ .  $\mathcal{AF}_4 = \{0000, 010(4,2)0102010(3)0102010, \dots\}$ .  $\mathcal{AF}_n$  for  $n \geq 4$  can be obtained by Theorem 7. Moreover, previous works on time-optimal jerk-limited trajectories like [11], [18], [19] are all devoted to study the first 8 switching law through model-based analysis, failing to enumerate complete  $\mathcal{AF}_3$ .

All augmented switching laws for any trajectory planning problem for high-order chain-of-integrators systems have been fully enumerated so far. In order words, the suboptimal solution of problem (1) with arbitrary initial states, terminal states, and full state constraints can be solved even by enumeration.

#### D. Calculation of Motion Time and Feasibility Verification

According to Definition 12 and 13,  $\forall S \in \mathcal{AF}_n, \dim S = n$ . Therefore, the motion time can be determined by a given initial state vector  $x_0$  and an augmented switching law  $S$ . Denote  $f : \mathbb{R}^n \times \mathbb{R} \times \mathbb{R} \rightarrow \mathbb{R}^n$  whose  $k$ -th component is

$$f_k(x, u, t) = \frac{1}{k!} u t^k + \sum_{i=1}^k \frac{1}{i!} x_{k-i} t^i. \quad (34)$$

$y = f(x, u, t)$  means system state vector moves from  $x$  to  $y$  under a constant control  $u$  by a period of time  $t$ . Next,

describe equations induced by a given  $S = s_1 s_2 \dots s_N \in \mathcal{AF}_n$ . Assume the system state vector reaches  $x_{m-1}$  before  $s_m$ . The control and time in stages of  $s_m$  are  $u_m$  and  $t_m$ , respectively.  $u_m$  and  $\text{sgn}(s_m)$  can be calculated by Theorem 3 and Theorem 5.

If  $s_m$  and  $s_{m+1}$  are system behaviors, or  $s_m$  and  $s_{m+1}$  are the virtual system behaviors, or  $m = N$ , then

$$\begin{cases} x_m = f(x_{m-1}, u_m, t_m), \\ x_{m,|s_m|} = \text{sgn}(s_m) M_{|s_m|}, \text{ if } |s_m| \neq 0, \\ x_{m,k} = 0, \text{ if } |s_m| \neq 0, k < |s_m|. \end{cases} \quad (35)$$

For  $s_l (s_{l+1} \dots s_{r-1}) s_r$ ,  $s_l$  and  $s_r$  are system behaviors, while  $(s_{l+1} \dots s_{r-1})$  is a virtual system behavior. According to Theorem 5-2,  $s_r = 0$ . Then,

$$\begin{cases} x_l = f(x_{l-1}, u_l, t_l), \\ x_{r-1} = f(x_{l-1}, u_l, t_{r-1}), \\ x_r = f(x_{r-1}, u_r, t_r), \\ x_{l,|s_l|} = \text{sgn}(s_l) M_{|s_l|}, \text{ if } |s_l| \neq 0, \\ x_{l,k} = 0, \text{ if } |s_l| \neq 0, k < |s_l|. \end{cases} \quad (36)$$

For  $s_{m-1} (s_m, d_m) s_{m+1}$ ,  $u_{m-1} = u_{m+1}$ , and  $u_m$  is not defined. Then,

$$\begin{cases} x_m = f(x_{m-2}, u_{m-1}, t_{m-1}), \\ x_{m,|s_m|} = \text{sgn}(s_m) M_{|s_m|}, \\ x_{m,|s_m|-k} = 0, k < d_m. \end{cases} \quad (37)$$

Finally,  $x_N$  is substituted as  $x_f$ .

Assume  $S \in \mathcal{AF}_n$  has  $N_0$  system behaviors,  $N_1$  virtual system behaviors, and  $N_2$  tangent markers. Then, the number of equations equals the number of variables, i.e.,  $(N_0 + N_1)(n + 1) - n$ .  $N_2$  satisfies  $\dim S = n$ .

Feasibility verification is trivial. On one hand,  $\forall m = 1, 2, \dots, N, t_m \geq 0$ . On the other hand,  $\forall m = 1, 2, \dots, N, \forall t \in [0, t_m], \forall k = 1, 2, \dots, n, |x_{m,k}(t)| \leq M_k$ , where  $x_{m,k}(t)$  is the system state after entering  $s_m$  for a period of time  $t$ . The latter feasibility condition can be verified by  $x_k(t) = f_k(x_p, u_m, t)$ , where  $x_p$  is the previous system state vector of  $s_m$  according to discussion above. Furthermore, checking  $|x_{m,k}(t)| \leq M_k$  at stationary points is enough [26].

Based on MIM in Section IV-A and enumeration of  $\mathcal{AF}_n$  in Section IV-C, a trajectory planning algorithm for high-order chain-of-integrators systems with arbitrary initial states, terminal states, and full state constraints are developed in Algorithm 1.

## V. NUMERICAL RESULTS AND DISCUSSION

### A. Simulation Setup

**Baselines.** To verify the performance of the proposed MIM method, i.e., Algorithm 1, simulation experiments for trajectories are conducted. The baselines are as follows.

- **Ruckig** [19] in community version: a jerk-limited time-optimal trajectory solver without position constraints.
- **SOCs** [32]: a time-optimal control method based on solving sequential convex second-order cone problems. The SOCps method is achieved by Gurobi [43].

---

**Algorithm 1:** Trajectory planning for high-order chain-of-integrators systems by MIM.

---

**Input:**  $n \in \mathbb{N}^*$ ,  $x_0, x_f \in \mathbb{R}^n$ ,  $M \in \mathbb{R}_{++} \times \mathbb{R}_{++}^n$ .

**Output:** Optimal control  $u = u^*(t)$  of problem (1).

**if**  $n = 1$  **then**

Solve the problem by (26) and **return**.

**end if**

**if**  $x_0$  is higher than  $\mathcal{F}_{n-1}(x_f; M^{0:(n-1)})$  **then**

Obtain  $u = \hat{u}^*(t)$  by  $\mathcal{P}(-x_0, -x_f, M)$ .

**return**  $u^*(t) = -\hat{u}^*(t)$ .

**end if**

**if**  $M_1 = M_2 = \dots = M_{n-1} = \infty$  **then**

Obtain  $x^*(t)$ ,  $u^*(t)$ ,  $t_f$  by solving  $n$  tandem (34).

**else**

$m \leftarrow \arg \max \{k < n : M_k < \infty\}$ .

Obtain  $x^{(1)}(t)$ ,  $t_{f1}$  by  $\mathcal{P}(x_0^{1:(n-1)}, M_m e_m, M^{0:m})$ .

**if**  $x_n^{(1)}(t_{f1})$  is lower than  $\mathcal{F}_{n-1}(x_f; M^{0:(n-1)})$  **then**

Obtain  $x^{(2)}(t)$  by  $\mathcal{P}(M_m e_m, x_f^{1:(n-1)}, M^{0:m})$ .

Obtain  $x^*(t)$  by connecting  $x^{(1)}$ ,  $x_m \equiv M_m$ ,  $x^{(2)}$ .

**else**

Solve  $t_1$  when  $x$  enters  $\mathcal{F}_{n-1}(x_f; M^{0:(n-1)})$ .

Obtain  $x^{(3)}(t)$  by  $\mathcal{P}(x^{1:(n-1)}(t_1), x_f^{1:(n-1)}, M^{0:m})$ .

Obtain  $x^*(t)$  by connecting  $x^{(1)}$ ,  $x^{(3)}$ .

**end if**

**end if**

**if**  $M_n < \infty$  **and**  $\exists t \in (0, t_f)$ ,  $|x_n^*(t)| > M_n$  **then**

**for**  $d \leftarrow 2, 4, \dots, 2 \lfloor \frac{n-1}{2} \rfloor$  **do**

**for**  $S \in \mathcal{AF}_d$  **do**

Obtain  $x = x^{(0)}(t)$ ,  $t_{f0}$  by  $S$ , where  $x$  moves from  $x_0$  to  $(n, d)$ ;

Obtain  $x = x^{(4)}(t)$  by  $\mathcal{P}(x(t_{f0}), x_f, M)$ .

Update the best feasible trajectory  $x^*(t)$  by connecting  $x^{(0)}$ ,  $x^{(4)}$ .

**end for**

**end for**

**end if**

---

- **Yop** [31]: a MATLAB toolbox for numerical optimal control problems based on CasADi [29] by direct methods.

The control period of Ruckig is set as 1 ms. The number of time points is set as 500 and 150 in SOCPs and Yop, respectively. In practice, if the number of time points is set more than 600 and 200 in SOCPs and Yop, respectively, then the computational time will increase obviously.

**Metrics.** For trajectory planning methods, the computational efficiency, the computational error, and the trajectory quality are significant performance metrics.

- The computational time  $T_c$ . All experiments are conducted in MATLAB 2021b on a computer with an AMD Ryzen 7 5800H @ 3.20 GHz processor.
- The error of the terminal states  $E_s$ . For a solved final

state vector  $\hat{x}_f$ ,  $E_s$  is defined in normalization as

$$E_s \triangleq \sqrt{\sum_{k=1}^n \left( \frac{x_{fk} - \hat{x}_{fk}}{M_k} \right)^2}. \quad (38)$$

- The success rate to obtain a feasible solution  $R_s$ . A result is determined to be successful if the states along the planned trajectories are feasible and  $E_s \leq 0.1$ .
- The normalized mean-squared error (MSE)  $E_m$  between the solved  $u = u(t)$  and the Bang-Singular-Bang control law [11] is defined to describe the trajectory quality. According to Proposition 1, the optimal control  $u^*(t) \in \{0, M_0, -M_0\}$  almost everywhere. Define

$$E_m \triangleq \sqrt{\frac{4}{M_0^2 t_f} \int_0^{t_f} u(t)^2 \wedge (|u(t)| - M_0)^2 dt}. \quad (39)$$

Then, the smaller  $E_m$  is, the closer  $u = u(t)$  is to a Bang-Singular-Bang control law, i.e., the better trajectory quality is. Specifically,  $E_m \in [0, 1]$ . Furthermore,  $E_m = 0$  if and only if  $\forall t \in [0, t_f]$ ,  $u(t) \in \{0, M_0, -M_0\}$  satisfies the Bang-Singular-Bang control law, while  $E_m = 1$  if and only if  $\forall t \in [0, t_f]$ ,  $|u(t)| = \frac{1}{2}M_0$ .

- The normalized total variation [41]  $T_v$  of the solved control is defined to describe the stability of the trajectory. For  $u(\frac{k}{n}t_f) = u_k$  with  $(n+1)$  waypoints, define

$$T_v \triangleq \frac{1}{2nM_0} \sum_{k=1}^n |u_k - u_{k-1}|. \quad (40)$$

Then, as  $T_v$  decreases, the trajectory exhibits increased oscillations, i.e., the stability of the trajectory decreases. Specifically,  $T_v \in [0, 1]$ . Furthermore,  $T_v = 0$  if and only if  $u_k \equiv \text{const}$ , while  $T_v = 1$  if and only if  $u_k = (-1)^k M_0$  or  $u_k = (-1)^{k-1} M_0$ .

## B. Numerical Results

Several trajectories planned by the proposed MIM and baselines are shown in Fig. 9 as examples, and the quantitative results of 100 jerk-limited trajectories and 100 snap-limited trajectories are shown in Fig. 10. Among them, 3rd order trajectories in Fig. 10 contain no tangent markers, since Ruckig in community version is not able to plan trajectories with position constraints. Furthermore, tangent markers occur in 3rd order trajectories only if the initial position and the terminal position are both close to boundaries, which occurs with a low probability.

It is noteworthy that the time-optimal problem (1) with an order  $n \geq 3$  is non-convex if it is solved in discretion directly [44]. Hence, discrete methods like Yop might fail to obtain an optimal trajectory, as shown in Fig. 9(a). Though SOCPs successfully transforms problem (1) into sequential convex problems, SOCPs might fail to obtain a feasible solution during iteration in some cases, as shown in Fig. 9(d). Furthermore, trajectories planned by Yop and SOCPs does not meet constraints (1d), causing failure as well. As shown in Fig. 10(a), Yop and SOCPs has a limited success rate, while Ruckig can plan all 3th order trajectories. Supported by



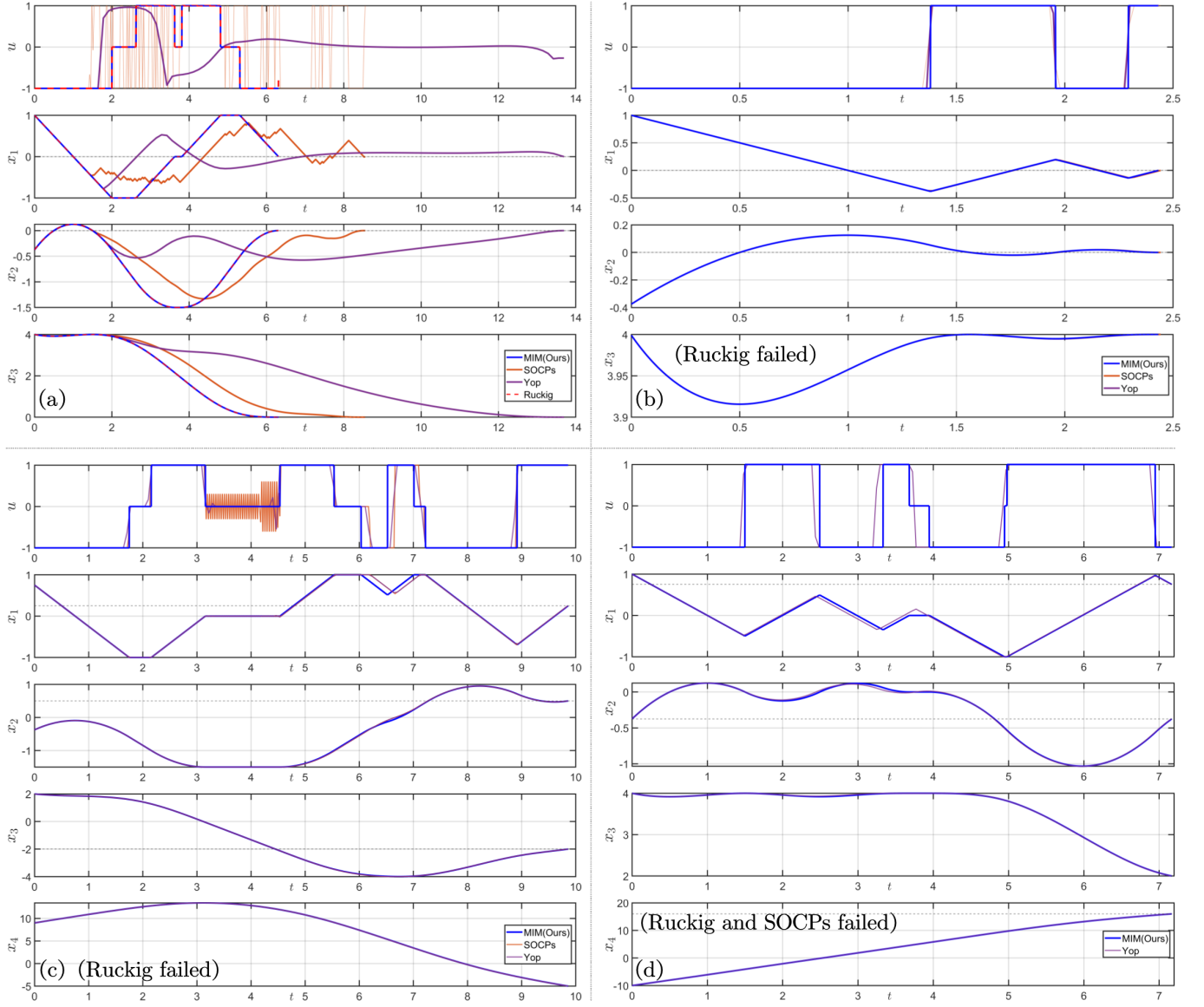


Fig. 9. Some trajectories planned by the proposed and baselines. (a) A jerk-limited trajectory represented by  $0102010$ .  $x_0 = (1, -0.375, 4)$ ,  $x_f = (0, 0, 0)$ ,  $M = (1, 1, 1.5, 4)$ . (b) A jerk-limited trajectory represented by  $00(3,2)000$ .  $x_0 = (1, -0.375, 3.999)$ ,  $x_f = (0, 0, 4)$ ,  $M = (1, 1, 1.5, 4)$ . (c) A snap-limited trajectory represented by  $0102010(3)0100$ .  $x_0 = (0.75, -0.375, 2, 9)$ ,  $x_f = (0.25, 0.5, -2, -5)$ ,  $M = (1, 1, 1.5, 4, 20)$ . (d) A snap-limited trajectory represented by  $00(3,2)00030100$ .  $x_0 = (1, -0.375, 4, -10)$ ,  $x_f = (0.75, -0.375, 2, 16)$ ,  $M = (1, 1, 1.5, 4, 20)$ . The trajectories of MIM and Ruckig almost coincide in (a), while  $x_3, x_4$  of all methods look to coincide.

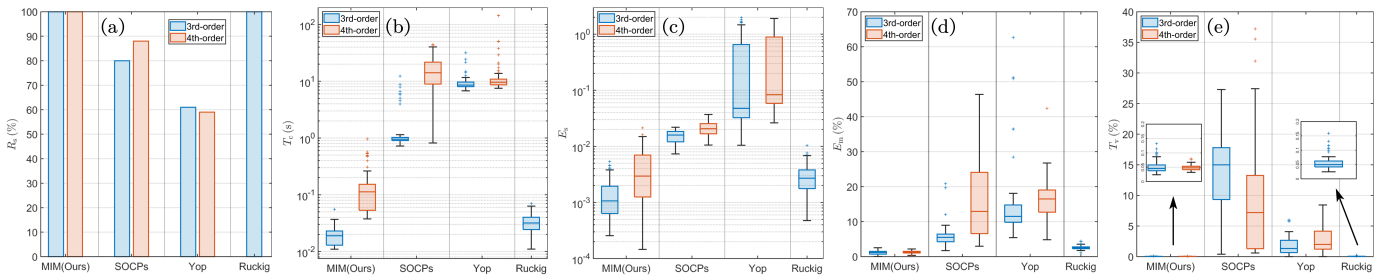


Fig. 10. Quantitative results of 100 3rd order trajectories and 100 4th order trajectories with random initial states and terminal states. (a) Success rate  $R_s$ . (b) Computational time  $T_c$ . (c) Error of terminal states  $E_s$ . (d) Normalized MSE  $E_m$  between input and the Bang-Singular-Bang control law. (e) Normalized total variation  $T_v$  of the planned control  $u$ . Ruckig is only applied in 3rd order trajectories because of disability to plan snap-limited trajectories.  $y$ -axes in (b) and (c) are in logarithmic scales.

theoretical results in Section III and Section IV, the proposed MIM succeeds in planning all randomly selected trajectories in 3rd and 4th order.

As shown in Fig. 10(c) and (d), the proposed MIM outperforms all baselines on computational time and computational accuracy. It can be observed that the proposed MIM achieves a computational time reduction of approximately 2 orders of magnitude compared to SOCPs and Yop, while improving computational accuracy by 90.8% (79.0%), 99.6% (99.0%), and 52.1% compared to SOCPs, Yop, and Ruckig, respectively, for 3rd order (4th order) problem in average. Specifically, MIM is not based on discrete time; hence, its computational efficiency keeps constant no matter what the control period is. On the contrary, as a real-time method, Ruckig requires longer computational time with a higher control frequency, but Ruckig is able to achieve a short computational time than the proposed MIM if its control frequency is set lower than 100 Hz, which is not conducive to precise motion control. Furthermore, the upper bound of the computational accuracy of MIM is determined only by the control frequency.

$E_m$  and  $T_v$  shown in Fig. 10(d) and (e) describe the trajectory quality.  $E_m$  and  $T_v$  of MIM and Ruckig are evidently lower than those of SOCPs and Yop. Therefore, the proposed MIM and Ruckig achieve much higher trajectory quality. Compared with SOCPs and Yop, trajectories generated by MIM are strict Bang-Singular-Bang. In addition to necessary switching, the input  $u(t)$  of the proposed MIM does not exhibit oscillations like those of SOCPs, as shown in Fig. 9(a) and (c). When the trajectory is short enough like Fig. 9(b), SOCPs has a short step width and can avoid oscillations. Quantitatively, MIM achieves a normalized MSE of control  $E_m$  that is 80.78% (92.3%), 91.9% (92.2%), and 57.2% lower than that of SOCPs, Yop, and Ruckig, respectively, for 3rd order (4th order) problems in average. Taking oscillations into consideration, MIM achieves a normalized total variation of control  $T_v$  that is 99.6% (99.5%), 97.1% (99.5%), and 10.1% lower than that of SOCPs, Yop, and Ruckig, respectively, for 3rd order (4th order) problems in average.

### C. Discussion

By comparing Algorithm 1 of 3rd order and Ruckig in community version [19] with 1-DOF, it can be examined that the proposed MIM plans the same trajectory with Ruckig for a given 3rd order problem. In conjunction with discussion in Section III, the proposed can plan strictly time-optimal trajectories in 3rd order and lower-order with full state constraints. Furthermore, it can be proved by induction that MIM plans optimal trajectories for  $n$ -th order problems when only  $|u| \leq M_0$  and  $|x_1| \leq M_1$  are active.

For 4th and higher-order problems, MIM plans quasi-optimal trajectories since the virtual system behavior in Definition 11 does not exist in time-optimal trajectories. Although the proposed MIM does not consider the chattering phenomenon in problem (1), MIM achieves terminal time closed to optimal solution, and avoids infinite times of chattering. For example, a set of typical kinematic parameters for the ultra-precision wafer stage are given in [45], where

$M_0 = 64\,000\text{ m/s}^4$ ,  $M_1 = 790\text{ m/s}^3$ ,  $M_2 = 10\text{ m/s}^2$ ,  $M_3 = 0.25\text{ m/s}^3$ , and  $M_4 = 0.02\text{ m}$ . Consider a position-to-position trajectory, i.e.,  $x_0 = -M_4 e_4$  and  $x_f = M_4 e_4$ . Then, MIM plans a suboptimal trajectory with terminal time  $t_{f,\text{MIM}} \approx 0.2100\text{ s}$ . According to Part II of this work [37], the optimal trajectory with chattering achieves terminal time  $t_f^*$ , where  $t_{f,\text{MIM}} - t_f^* \approx 29.2\text{ ns}$ . So MIM achieves a relative error of 0.14% in terminal time compared to the optimal solution, and is able to avoid chattering; note that the control period is usually  $200\text{ }\mu\text{s} \gg 29.2\text{ ns}$ . Therefore, the MIM-trajectory is near-optimal and practical for high-order problems.

It is meaningful to strictly solve the time-optimal problem (1) in further study, which would be a landmark achievement in the optimal control theory. To the best of our knowledge, the theoretical framework established in Section III provides unprecedented insights into problem (1), surpassing current literature. Therefore, it is believed that the theoretical framework established in Section III would be a noteworthy mathematical tool for the final resolution of the time-optimal problem (1).

## VI. CONCLUSION

This paper has set out to theoretically study a classical and challenging problem in the optimal control theory domain, i.e., the time-optimal control problem for high-order chain-of-integrators systems with full state constraints and arbitrary terminal states. To this end, this paper establishes a novel notation system and theoretical framework, providing the switching manifold for high-order problems in the form of switching laws. The framework derives properties of switching laws on signs as well as dimension and reasons a definite condition of augmented switching laws. Guided by the developed framework, a trajectory planning method named the manifold-intercept method (MIM) has been proposed, outperforming all baselines on computational time, computational accuracy, and trajectory quality by a large gap. The proposed MIM can achieve time-optimal trajectories for 3rd order or lower-order problems with full state constraints. MIM can also plan near-time-optimal trajectories efficiently and accurately with negligible extra motion time compared to time-optimal trajectories that are lack of mature algorithms currently, avoiding chattering phenomenon that impedes numerical computation in practice.

## ACKNOWLEDGMENT

The authors would like to thank the anonymous reviewers for their valuable comments and suggestions, to thank Yujie Lin and Hui Ma for their expertise in differential geometry, and to thank Zongying Shi for her expertise in optimal control. This work was supported by the National Natural Science Foundation of China under Grant 51922059 and 52205532.

## REFERENCES

- [1] W. Wang, C. Hu, K. Zhou, S. He, and L. Zhu, "Local asymmetrical corner trajectory smoothing with bidirectional planning and adjusting algorithm for cnc machining," *Robotics and Computer-Integrated Manufacturing*, vol. 68, p. 102058, 2021.

- [2] Z. Wang, R. Zhou, C. Hu, and Y. Zhu, "Real-time iterative compensation based contouring control method for polar coordinate motion systems," *IEEE/ASME Transactions on Mechatronics*, vol. 27, no. 5, pp. 3517–3526, 2022.
- [3] Y. Wang, J. Wang, Y. Li, C. Hu, and Y. Zhu, "Learning latent object-centric representations for visual-based robot manipulation," in *2022 International Conference on Advanced Robotics and Mechatronics (ICARM)*. IEEE, 2022, pp. 138–143.
- [4] G. Zhao and M. Zhu, "Pareto optimal multirobot motion planning," *IEEE Transactions on Automatic Control*, vol. 66, no. 9, pp. 3984–3999, 2020.
- [5] J. Wang, C. Hu, Y. Wang, and Y. Zhu, "Dynamics learning with object-centric interaction networks for robot manipulation," *IEEE Access*, vol. 9, pp. 68 277–68 288, 2021.
- [6] C. Ni, M. Zhang, Y. Zhu, C. Hu, S. Ding, and Z. Jia, "Sinusoidal phase-modulating interferometer with ellipse fitting and a correction method," *Applied Optics*, vol. 56, no. 13, pp. 3895–3899, 2017.
- [7] M. Li, Y. Zhu, K. Yang, L. Yang, C. Hu, and H. Mu, "Convergence rate oriented iterative feedback tuning with application to an ultraprecision wafer stage," *IEEE Transactions on Industrial Electronics*, vol. 66, no. 3, pp. 1993–2003, 2018.
- [8] S. Güler, B. Fidan, S. Dasgupta, B. D. Anderson, and I. Shames, "Adaptive source localization based station keeping of autonomous vehicles," *IEEE Transactions on Automatic Control*, vol. 62, no. 7, pp. 3122–3135, 2016.
- [9] Y. Wang, C. Hu, Z. Wang, S. Lin, Z. Zhao, W. Zhao, K. Hu, Z. Huang, Y. Zhu, and Z. Lu, "Optimization-based non-equidistant toolpath planning for robotic additive manufacturing with non-underfill orientation," *Robotics and Computer-Integrated Manufacturing*, vol. 84, p. 102599, 2023.
- [10] Y. Wang, C. Hu, Z. Wang, S. Lin, Z. Zhao, and Y. Zhu, "Slice extension for high-quality hybrid additive-subtractive manufacturing," in *IECON 2023-49th Annual Conference of the IEEE Industrial Electronics Society*. IEEE, 2023, pp. 1–6.
- [11] S. He, C. Hu, Y. Zhu, and M. Tomizuka, "Time optimal control of triple integrator with input saturation and full state constraints," *Automatica*, vol. 122, p. 109240, 2020.
- [12] R. F. Hartl, S. P. Sethi, and R. G. Vickson, "A survey of the maximum principles for optimal control problems with state constraints," *SIAM review*, vol. 37, no. 2, pp. 181–218, 1995.
- [13] E. B. Lee and L. Markus, "Foundations of optimal control theory," Minnesota Univ Minneapolis Center For Control Sciences, Tech. Rep., 1967.
- [14] G. Bartolini, S. Pillosu, A. Pisano, E. Usai *et al.*, "Time-optimal stabilization for a third-order integrator: A robust state-feedback implementation," *Lecture notes in control and information sciences*, pp. 131–144, 2002.
- [15] N. Marchand, A. Hably, and A. Chemori, "Global stabilization with low computational cost of the discrete-time chain of integrators by means of bounded controls," *IEEE Transactions on Automatic Control*, vol. 52, no. 5, pp. 948–952, 2007.
- [16] Z. Ma and S. Zou, *Optimal Control Theory: The Variational Method*. Springer, 2021.
- [17] R. Haschke, E. Weitnauer, and H. Ritter, "On-line planning of time-optimal, jerk-limited trajectories," in *2008 IEEE/RSJ International Conference on Intelligent Robots and Systems*. IEEE, 2008, pp. 3248–3253.
- [18] T. Kröger, "Opening the door to new sensor-based robot applications—the reflexes motion libraries," in *2011 IEEE International Conference on Robotics and Automation*. IEEE, 2011, pp. 1–4.
- [19] L. Berscheid and T. Kröger, "Jerk-limited real-time trajectory generation with arbitrary target states," in *Robotics: Science and Systems*, 2021.
- [20] S. He, C. Hu, S. Lin, Y. Zhu, and M. Tomizuka, "Real-time time-optimal continuous multi-axis trajectory planning using the trajectory index coordination method," *ISA transactions*, vol. 131, pp. 639–649, 2022.
- [21] Y. Gao, K. H. Johansson, and L. Xie, "Computing probabilistic controlled invariant sets," *IEEE Transactions on Automatic Control*, vol. 66, no. 7, pp. 3138–3151, 2020.
- [22] U. Walther, T. T. Georgiou, and A. Tannenbaum, "On the computation of switching surfaces in optimal control: A grobner basis approach," *IEEE Transactions on Automatic Control*, vol. 46, no. 4, pp. 534–540, 2001.
- [23] E. Khmelnitsky and M. Caramanis, "One-machine n-part-type optimal setup scheduling: analytical characterization of switching surfaces," *IEEE Transactions on Automatic Control*, vol. 43, no. 11, pp. 1584–1588, 1998.
- [24] I. M. Mitchell, A. M. Bayen, and C. J. Tomlin, "A time-dependent hamilton-jacobi formulation of reachable sets for continuous dynamic games," *IEEE Transactions on automatic control*, vol. 50, no. 7, pp. 947–957, 2005.
- [25] F. Tahir and I. M. Jaimoukha, "Low-complexity polytopic invariant sets for linear systems subject to norm-bounded uncertainty," *IEEE Transactions on Automatic Control*, vol. 60, no. 5, pp. 1416–1421, 2014.
- [26] L. Doesser, P. Nilsson, A. D. Ames, and R. M. Murray, "Invariant sets for integrators and quadrotor obstacle avoidance," in *2020 American Control Conference (ACC)*. IEEE, 2020, pp. 3814–3821.
- [27] M. Yury, "Quasi-time-optimal control of third-order integrators with phase constraints," in *2016 International Conference Stability and Oscillations of Nonlinear Control Systems (Pyatnitskiy's Conference)*. IEEE, 2016, pp. 1–4.
- [28] H. Robbins, "Junction phenomena for optimal control with state-variable inequality constraints of third order," *Journal of Optimization Theory and Applications*, vol. 31, pp. 85–99, 1980.
- [29] J. A. Andersson, J. Gillis, G. Horn, J. B. Rawlings, and M. Diehl, "Casadi: a software framework for nonlinear optimization and optimal control," *Mathematical Programming Computation*, vol. 11, pp. 1–36, 2019.
- [30] Y. Nie, O. Faqir, and E. C. Kerrigan, "Iclocs2: Try this optimal control problem solver before you try the rest," in *2018 UKACC 12th international conference on control (CONTROL)*. IEEE, 2018, pp. 336–336.
- [31] V. Leek, "An optimal control toolbox for matlab based on casadi," 2016.
- [32] M. Leomanni, G. Costante, and F. Ferrante, "Time-optimal control of a multidimensional integrator chain with applications," *IEEE Control Systems Letters*, vol. 6, pp. 2371–2376, 2022.
- [33] K. Erkorkmaz and Y. Altintas, "High speed cnc system design. part i: jerk limited trajectory generation and quintic spline interpolation," *International Journal of machine tools and manufacture*, vol. 41, no. 9, pp. 1323–1345, 2001.
- [34] L. Dai, X. Li, Y. Zhu, M. Zhang, and C. Hu, "The generation mechanism of tracking error during acceleration or deceleration phase in ultraprecision motion systems," *IEEE Transactions on Industrial Electronics*, vol. 66, no. 9, pp. 7109–7119, 2018.
- [35] B. Ezair, T. Tassa, and Z. Shiller, "Planning high order trajectories with general initial and final conditions and asymmetric bounds," *The International Journal of Robotics Research*, vol. 33, no. 6, pp. 898–916, 2014.
- [36] E. Oland and R. Kristiansen, "Controlling a chain of integrators with constrained actuation using exponential activation functions," in *2019 IEEE 10th International Conference on Mechanical and Aerospace Engineering (ICMAE)*. IEEE, 2019, pp. 258–261.
- [37] Y. Wang, C. Hu, Z. Li, Y. Lin, S. Lin, S. He, and Y. Zhu, "Time-optimal control for high-order chain-of-integrators systems with full state constraints and arbitrary terminal states (part ii)," *to appear*.
- [38] L. Berscheid, "Ruckig - motion generation for robots and machines," <https://ruckig.com/>, 2023.
- [39] C. Fox, *An introduction to the calculus of variations*. Courier Corporation, 1987.
- [40] D. H. Jacobson, M. M. Lele, and J. L. Speyer, "New necessary conditions of optimality for control problems with state-variable inequality constraints," *Journal of mathematical analysis and applications*, vol. 35, no. 2, pp. 255–284, 1971.
- [41] E. M. Stein and R. Shakarchi, *Real analysis: measure theory, integration, and Hilbert spaces*. Princeton University Press, 2009.
- [42] R. Bellman, "On the theory of dynamic programming," *Proceedings of the national Academy of Sciences*, vol. 38, no. 8, pp. 716–719, 1952.
- [43] L. Gurobi Optimization, "Gurobi optimizer reference manual," <https://www.gurobi.com>, 2023.
- [44] F. Debruyere, W. Van Loock, G. Pipeleers, Q. T. Dinh, M. Diehl, J. De Schutter, and J. Swevers, "Time-optimal path following for robots with convex-concave constraints using sequential convex programming," *IEEE Transactions on Robotics*, vol. 29, no. 6, pp. 1485–1495, 2013.
- [45] M. Li, Y. Zhu, K. Yang, and C. Hu, "A data-driven variable-gain control strategy for an ultra-precision wafer stage with accelerated iterative parameter tuning," *IEEE Transactions on Industrial Informatics*, vol. 11, no. 5, pp. 1179–1189, 2015.

APPENDIX A  
PROOF OF INDEPENDENCE OF EQUATIONS IN THEOREM 2

Given the terminal state vector  $\mathbf{x}_f \in \mathbb{R}^n$ , the constraints  $\mathbf{M} = (M_0, M_1, \dots, M_n) \in \mathbb{R}_{++} \times \overline{\mathbb{R}}_{++}^n$ , and a switching law  $S = s_1 s_2 \dots s_N$ , we need to prove that if  $\exists \mathbf{x}_0 \in \mathbb{R}^n$ , s.t.  $S \in \mathcal{P}(\mathbf{x}_0, \mathbf{x}_f; \mathbf{M})$ , then the dimension of the manifold represented by  $S$  is

$$\dim S = N - \sum_{i=1}^N |s_i|. \quad (41)$$

Before proving, we need to prove that  $\mathbf{J}$  has full row rank. The condition in Theorem 2 is equivalent to the following condition.

**Condition 1.**  $\forall i = 1, 2, \dots, N$ , the following conditions hold:

- 1) If  $\exists 1 \leq j < i$ , s.t.,  $|s_j| \geq |s_i|$ , then  $\sum_{k=j+1}^i |s_k| < i - j$ .
- 2) If  $\exists i < j \leq N$ , s.t.,  $|s_j| \geq |s_i|$ , then  $\sum_{k=i}^{j-1} |s_k| < j - i$ .
- 3) If  $|s_i| > 0$  and  $\forall i < j \leq N$ ,  $|s_j| < |s_i|$ , then  $\sum_{k=i}^N |s_k| \leq N - i$ .

Condition 1 is naturally introduced to avoid some special cases. To understand Condition 1-1, we consider the trajectory  $\mathbf{x}_{1:|s_i|}(t)$ ,  $t \in [t_j, t_i]$ . It is evident that  $\mathbf{x}_{1:|s_i|}(t_i) = M_{|s_i|} \text{sgn}(s_i) \mathbf{e}_{|s_i|}$ . If  $|s_j| = |s_i|$ , then  $\mathbf{x}_{1:|s_i|}(t_j) = M_{|s_i|} \text{sgn}(s_j) \mathbf{e}_{|s_i|}$ ; if  $|s_j| > |s_i|$ , then  $\mathbf{x}_{1:|s_i|}(t_j) = \mathbf{0}$ . Then, the “degree of freedom” should not be smaller than  $|s_i|$ , i.e., the number of variables should not be less than the number of equations. Hence, it is assumed that  $\sum_{k=j+1}^i |s_k| < i - j$ . Similar analysis can be applied to Condition 1-2. For Condition 1-3, it does not hold only when the terminal state vector  $\mathbf{x}_f$  is in a zero-measure set. For example, if  $|s_N| \neq 0$ , then  $\mathbf{x}_f$  satisfies  $\mathbf{x}_{f,1:|s_N|} = \text{sgn}(s_N) M_{|s_N|}$ ; however, once  $\mathbf{x}_f$  is disturbed slightly resulting in  $\hat{\mathbf{x}}_f$ , then except of a zero-measure set in the neighborhood of  $\mathbf{x}_f$ , the switching law should with terminal states  $\hat{\mathbf{x}}_f$  should end with  $s_N$  and  $|s_N|$  zeros.

We assume  $\mathbf{x}_i = (x_{i,k})_{k=1}^n \in \mathbb{R}^n$ ,  $i = 0, 1, \dots, N$  and  $t_i \geq 0$ ,  $i = 1, 2, \dots, N$ .  $\mathbf{x}_{i-1}$  moves to  $\mathbf{x}_i$  after time  $t_i$  under the system behavior  $s_i$ ,  $\forall i = 1, 2, \dots, N$ . Among them, the terminal state vector  $\mathbf{x}_N = \mathbf{x}_f$  is given, while  $\mathbf{x}_i$ ,  $i = 0, 1, \dots, N$  and  $t_i$ ,  $i = 1, 2, \dots, N$  are variables. By Condition 1-3,  $|s_N| = 0$ .

Under the system behavior  $s_i$ , the control  $u \equiv u_i$ , where

$$x_{i,0} \triangleq u_i = \begin{cases} \text{sgn}(s_i) M_0, & |s_i| = 0 \\ 0, & |s_i| \neq 0 \end{cases}. \quad (42)$$

Denote

$$\mathbf{X} = \begin{bmatrix} \mathbf{x}_0 \\ \mathbf{x}_1 \\ \vdots \\ \mathbf{x}_{N-1} \\ t_1 \\ t_2 \\ \vdots \\ t_N \end{bmatrix} \in \mathbb{R}^{N(n+1)}. \quad (43)$$

Then, we have the following constraints:

$$f_{(i-1)n+k}(\mathbf{X}) = \sum_{j=1}^k \frac{1}{(k-j)!} x_{i-1,j} t_i^{k-j} + \frac{1}{k!} u_i t_i^k - x_{i,k} = 0, \quad i = 1, 2, \dots, N, \quad k = 1, 2, \dots, n, \quad (44a)$$

$$f_{Nn+\sum_{j=1}^{i-1} |s_j|+k}(\mathbf{X}) = x_{i,k} = 0, \quad i = 1, 2, \dots, N-1, \quad k = 1, 2, \dots, |s_i| - 1, \quad (44b)$$

$$f_{Nn+\sum_{j=1}^i |s_j|}(\mathbf{X}) = x_{i,k} - \text{sgn}(s_i) M_{|s_i|} = 0, \quad i = 1, 2, \dots, N-1. \quad (44c)$$

Among them,  $x_{N,k} = 0$  for  $k < |s_N|$  and  $x_{N,|s_N|} = \text{sgn}(s_N) M_{|s_N|}$  are guaranteed by the given  $\mathbf{x}_f$  since  $\exists \mathbf{x}_0 \in \mathbb{R}^n$ , s.t.  $S \in \mathcal{P}(\mathbf{x}_0, \mathbf{x}_f; \mathbf{M})$ . Naturally, according to (42),  $x_{N-1,k} = 0$  for  $k < |s_N|$  and  $x_{N-1,|s_N|} = \text{sgn}(s_N) M_{|s_N|}$ .

Denote the above constraints as  $\mathbf{f}(\mathbf{X}) = \mathbf{0}$ . Since  $\exists \mathbf{x}_0 \in \mathbb{R}^n$ , s.t.  $S \in \mathcal{P}(\mathbf{x}_0, \mathbf{x}_f; \mathbf{M})$ , the system of equations  $\mathbf{f}(\mathbf{X}) = \mathbf{0}$  has at least one solution, denoted as

$$\mathbf{X}^* = \begin{bmatrix} \mathbf{x}_0^* \\ \mathbf{x}_1^* \\ \vdots \\ \mathbf{x}_{N-1}^* \\ t_1^* \\ t_2^* \\ \vdots \\ t_N^* \end{bmatrix} \in \mathbb{R}^{N(n+1)}. \quad (45)$$

Then, we try to calculate  $\left. \frac{d\mathbf{f}}{d\mathbf{X}} \right|_{\mathbf{X}^*}$ , i.e., the Jacobi matrix of  $\mathbf{f}(\mathbf{X})$  at  $\mathbf{X}^*$ . For (44a),  $\forall i = 1, 2, \dots, N$ ,

$$\left. \frac{\partial \mathbf{f}_{((i-1)n+1):in}}{\partial \mathbf{x}_{i-1}} \right|_{\mathbf{X}^*} = \Phi_n(t_i^*), \quad (46a)$$

$$\left. \frac{\partial \mathbf{f}_{((i-1)n+1):in}}{\partial \mathbf{x}_i} \right|_{\mathbf{X}^*} = -\mathbf{I}_n, \quad i < N, \quad (46b)$$

$$\left. \frac{\partial \mathbf{f}_{((i-1)n+1):in}}{\partial \mathbf{x}_j} \right|_{\mathbf{X}^*} = \mathbf{0}_{n \times n}, \quad j \neq i, i-1, \quad (46c)$$

$$\left. \frac{\partial \mathbf{f}_{((i-1)n+1):in}}{\partial t_i} \right|_{\mathbf{X}^*} = \left( \sum_{j=0}^{k-1} \frac{1}{(k-j)!} x_{i-1,j}^* t_i^{*k-j} \right)_{k=1}^n \stackrel{(44a)}{=} \mathbf{x}_{i,0:(n-1)}^*, \quad (46d)$$

$$\left. \frac{\partial \mathbf{f}_{((i-1)n+1):in}}{\partial t_j} \right|_{\mathbf{X}^*} = \mathbf{0}_{n \times 1}, \quad j \neq i. \quad (46e)$$

Among them, for a vector  $\mathbf{x} = (x_i)_{i=1}^n$ ,  $\mathbf{x}_{a:b} \triangleq \mathbf{x} = (x_i)_{i=a}^b$ . For a matrix  $\mathbf{A} = ((a_{ij})_{i=1}^m)_{j=1}^n$ ,  $\mathbf{A}_{a:b,c:d} \triangleq ((a_{ij})_{i=a}^b)_{j=c}^d$ .  $\mathbf{0}_{m \times n} = ((0)_{i=1}^m)_{j=1}^n$ . In (46a),

$$\Phi_a(t) \triangleq \begin{bmatrix} 1 & & & & \\ t & 1 & & & \\ \frac{t^2}{2} & t & 1 & & \\ \vdots & \vdots & \vdots & \ddots & \\ \frac{t^{a-1}}{(a-1)!} & \frac{t^{a-2}}{(a-2)!} & \frac{t^{a-3}}{(a-3)!} & \cdots & 1 \end{bmatrix}, \quad a \in \mathbb{N}^*, \quad (47)$$

is invertible.  $\forall t \in \mathbb{R}$ ,  $a \in \mathbb{N}^*$ ,  $\det \Phi_a(t) = 1$ .

For (44b) and (44c),  $\forall i = 1, 2, \dots, N-1$ ,

$$\left. \frac{\partial \mathbf{f}_{(Nn+\sum_{j=1}^{i-1}|s_j|+1):(Nn+\sum_{j=1}^i|s_j|)}}{\partial \mathbf{x}_i} \right|_{\mathbf{X}^*} = \mathbf{I}_{|s_i| \times n}, \quad (48a)$$

$$\left. \frac{\partial \mathbf{f}_{(Nn+\sum_{j=1}^{i-1}|s_j|+1):(Nn+\sum_{j=1}^i|s_j|)}}{\partial \mathbf{x}_j} \right|_{\mathbf{X}^*} = \mathbf{0}_{|s_i| \times n}, \quad j \neq i, \quad (48b)$$

$$\left. \frac{\partial \mathbf{f}_{(Nn+\sum_{j=1}^{i-1}|s_j|+1):(Nn+\sum_{j=1}^i|s_j|)}}{\partial t_j} \right|_{\mathbf{X}^*} = \mathbf{0}_{|s_i| \times 1}, \quad j = 1, 2, \dots, N. \quad (48c)$$

Among them,  $\mathbf{I}_{m \times n} = ((\delta_{ij})_{i=1}^m)_{j=1}^n$ . Specifically, if  $m \leq n$ ,  $\mathbf{I}_{m \times n} = [\mathbf{I}_m, \mathbf{0}_{m \times (n-m)}]$ . If  $m > n$ ,  $\mathbf{I}_{m \times n} = \mathbf{I}_{n \times n}^\top$ .



Therefore, the Jacobi matrix of  $\mathbf{f}(\mathbf{X})$  at  $\mathbf{X}^*$ , denoted as  $\mathbf{J} = \left. \frac{d\mathbf{f}}{d\mathbf{X}} \right|_{\mathbf{X}^*}$ , is

$$\mathbf{J} = \begin{bmatrix} \Phi_n(t_1^*) & -\mathbf{I}_n & & & \mathbf{x}_{1,0:(n-1)}^* & & & \\ & \Phi_n(t_2^*) & -\mathbf{I}_n & & & \mathbf{x}_{2,0:(n-1)}^* & & \\ & & \ddots & \ddots & & & \ddots & \\ & & & \Phi_n(t_{N-1}^*) & -\mathbf{I}_n & & & \mathbf{x}_{N-1,0:(n-1)}^* \\ & & & & \Phi_n(t_N^*) & & & \mathbf{x}_{N,0:(n-1)}^* \\ & \mathbf{I}_{|s_1| \times n} & & & & & & \\ & & \mathbf{I}_{|s_2| \times n} & & & & & \\ & & & \ddots & & & & \\ & & & & \mathbf{I}_{|s_{N-1}| \times n} & & & \end{bmatrix}. \quad (49)$$

**Theorem 8.** *If Condition 1 holds, then  $\mathbf{J}$  in (49) has full row rank.*

Due to the complexity of the proof of Theorem 3.2.1, we relegate the demonstration of this theorem to the conclusion of the response to this comment.

**Lemma 2.**  $n \in \mathbb{N}^*$ . Denote  $\phi_k(t) \triangleq \frac{t^{k-1}}{(k-1)!}$ . Denote  $\phi_n(t) \triangleq (\phi_k(t))_{k=1}^n \in \mathbb{R}^n$ .  $\Phi_n$  is defined in (47). Assume  $\mathbf{x} = \mathbf{x}(t) = (x_k(t))_{k=1}^n$  is the solution of the initial value problem

$$\begin{cases} \dot{x}_1(t) = 0, \quad t \in \mathbb{R}, \\ \dot{x}_{k+1}(t) = x_k(t), \quad k = 1, 2, \dots, n-1, \quad t \in \mathbb{R}, \\ \mathbf{x}(t_0) = \mathbf{x}_0. \end{cases}$$

Among them,  $t_0 \in \mathbb{R}$  and  $\mathbf{x}_0 = (x_{0,k})_{k=1}^n \in \mathbb{R}^n$  are given. Then,

- 1)  $\phi_n(0) = \mathbf{e}_1 \in \mathbb{R}^n$ ,  $\Phi_n(0) = \mathbf{I}_n$ .
- 2)  $\forall t_1, t_2 \in \mathbb{R}$ ,  $\Phi_n(t_2) \phi_n(t_1) = \phi_n(t_1 + t_2)$ ,  $\Phi_n(t_1) \Phi_n(t_2) = \Phi_n(t_2) \Phi_n(t_1) = \Phi_n(t_1 + t_2)$ .
- 3)  $\forall t \in \mathbb{R}$ ,  $\Phi_n(t)$  is invertible, and  $\Phi_n^{-1}(t) = \Phi_n(-t)$ .
- 4)  $\forall t \in \mathbb{R}$ ,  $\mathbf{x}(t) = \Phi_n(t - t_0) \mathbf{x}_0$ .

*Proof.* Lemma 2.1 holds evidently.

Now we prove Lemma 2.2.  $\forall t_1, t_2 \in \mathbb{R}$ ,  $\Phi_n(t_k) = \left( \left( \frac{t_k^{i-j}}{(i-j)!} \delta_{i \geq j} \right)_{i=1}^n \right)_{j=1}^n$ ,  $k = 1, 2$ . Therefore,

$$\begin{aligned} \Phi_n(t_1) \Phi_n(t_2) &= \left( \left( \frac{t_1^{i-k}}{(i-k)!} \delta_{i \geq k} \right)_{i=1}^n \right)_{k=1}^n \left( \left( \frac{t_2^{k-j}}{(k-j)!} \delta_{k \geq j} \right)_{k=1}^n \right)_{j=1}^n \\ &= \left( \left( \sum_{k=1}^n \frac{t_1^{i-k}}{(i-k)!} \delta_{i \geq k} \frac{t_2^{k-j}}{(k-j)!} \delta_{k \geq j} \right)_{i=1}^n \right)_{j=1}^n \\ &= \left( \left( \sum_{k=j}^i \frac{t_1^{i-k} t_2^{k-j}}{(i-k)! (k-j)!} \delta_{i \geq j} \right)_{i=1}^n \right)_{j=1}^n \\ &= \left( \left( \frac{\delta_{i \geq j}}{(i-j)!} \sum_{k=0}^{i-j} \frac{(i-j)!}{(i-j-k)! k!} t_1^{i-j-k} t_2^k \right)_{i=1}^n \right)_{j=1}^n \\ &= \left( \left( \frac{(t_1 + t_2)^{i-j}}{(i-j)!} \delta_{i \geq j} \right)_{i=1}^n \right)_{j=1}^n \\ &= \Phi_n(t_1 + t_2). \end{aligned}$$

So  $\Phi_n(t_1) \Phi_n(t_2) = \Phi_n(t_2) \Phi_n(t_1) = \Phi_n(t_1 + t_2)$  for the same reason. Note that  $\phi_n(t_2)$  and  $\phi_n(t_1 + t_2)$  are the first row of  $\Phi_n(t_2)$  and  $\Phi_n(t_1 + t_2)$ , respectively. Therefore,  $\Phi_n(t_2) \phi_n(t_1) = \phi_n(t_1 + t_2)$ . Lemma 2.2 holds.

By Lemma 2.2,  $\forall t \in \mathbb{R}$ ,  $\Phi_n(t) \Phi_n^{-1}(t) = \Phi_n^{-1}(t) \Phi_n(t) = \mathbf{I}_n$ . Therefore,  $\Phi_n^{-1}(t) = \Phi_n(-t)$ . Lemma 2.3 holds.

Next we prove Lemma 2.4. By solving the initial value problem,  $\forall t \in \mathbb{R}$ ,  $k = 1, 2, \dots, n$ ,  $x_k(t) = \sum_{i=0}^k \frac{(t-t_0)^i}{i!} x_{k-i}(t_0)$ . Therefore,  $\mathbf{x}(t) = \Phi_n(t - t_0) \mathbf{x}_0$ . Lemma 2.4 holds.  $\square$

**Lemma 3.**  $n \in \mathbb{N}^*$ . Denote  $\hat{\phi}_k(t) \triangleq t^{k-1}$ . Denote  $\hat{\phi}_n(t) \triangleq \left(\hat{\phi}_k(t)\right)_{k=1}^n$ . Denote  $\hat{\Phi}_n(t) = \left(\left(\frac{i!}{j!(i-j)!}t^{i-j}\right)_{i=1}^n\right)_{j=1}^n$ , i.e.,

$$\hat{\phi}_n(t) \triangleq \begin{bmatrix} 1 \\ t \\ t^2 \\ \vdots \\ t^{n-1} \end{bmatrix}, \quad \hat{\Phi}_n(t) \triangleq \begin{bmatrix} 1 & & & & \\ 2t & 1 & & & \\ 3t^2 & 3t & 1 & & \\ \vdots & \vdots & \vdots & \ddots & \\ nt^{n-1} & \frac{n(n-1)}{2}t^{n-2} & \frac{n(n-1)(n-2)}{6}t^{n-3} & \dots & 1 \end{bmatrix}.$$

Then,

- 1)  $\hat{\phi}_n(0) = \mathbf{e}_1 \in \mathbb{R}^n$ ,  $\hat{\Phi}_n(0) = \mathbf{I}_n$ .
- 2)  $\forall t_1, t_2 \in \mathbb{R}$ ,  $\hat{\Phi}_n(t_2)\hat{\phi}_n(t_1) = \hat{\phi}_n(t_1+t_2)$ ,  $\hat{\Phi}_n(t_1)\hat{\Phi}_n(t_2) = \hat{\Phi}_n(t_2)\hat{\Phi}_n(t_1) = \hat{\Phi}_n(t_1+t_2)$ .
- 3)  $\forall t \in \mathbb{R}$ ,  $\hat{\Phi}_n(t)$  is invertible, and  $\hat{\Phi}_n^{-1}(t) = \hat{\Phi}_n(-t)$ .

*Proof.* Lemma 3.1 holds evidently. Note that  $\hat{\phi}_n(t) = \mathbf{C}\phi_n(t)$ ,  $\hat{\Phi}_n(t) = \mathbf{C}\Phi_n(t)\mathbf{C}^{-1}$ , where

$$\mathbf{C} = \begin{bmatrix} 0! & & & \\ & 1! & & \\ & & \ddots & \\ & & & (n-1)! \end{bmatrix}.$$

According to Lemma 2.2,  $\forall t_1, t_2 \in \mathbb{R}$ ,

$$\hat{\Phi}_n(t_2)\hat{\phi}_n(t_1) = \mathbf{C}\Phi_n(t_2)\mathbf{C}^{-1}\mathbf{C}\phi_n(t_1) = \mathbf{C}\phi_n(t_1+t_2) = \hat{\phi}_n(t_1+t_2).$$

Similarly,

$$\hat{\Phi}_n(t_1)\hat{\Phi}_n(t_2) = \mathbf{C}\Phi_n(t_1)\mathbf{C}^{-1}\mathbf{C}\Phi_n(t_2)\mathbf{C}^{-1} = \mathbf{C}\Phi_n(t_1+t_2)\mathbf{C}^{-1} = \hat{\Phi}_n(t_1+t_2).$$

So Lemma 3.2 holds. Furthermore,  $\forall t \in \mathbb{R}$ ,  $\hat{\Phi}_n(t)\hat{\Phi}_n(-t) = \hat{\Phi}_n(-t)\hat{\Phi}_n(t) = \hat{\Phi}_n(0) = \mathbf{I}_n$ ; hence, Lemma 3.3 holds.  $\square$

**Lemma 4.**  $\forall \{T_k\}_{k=1}^\infty \subset \mathbb{R}$  is monotonically strictly increasing, i.e.,  $T_1 < T_2 < T_3 < \dots$ , define

$$D_{n,m,p} = D_{n,m} \left( (T_k)_{k=p}^{m+p} \right) \triangleq \begin{cases} 1, & m=0, n=0, \\ T_p^n, & m=0, n \geq 1, \\ \frac{D_{n,m-1} \left( (T_k)_{k=p+1}^{m+p} \right) - D_{n,m-1} \left( (T_k)_{k=p}^{m+p-1} \right)}{T_{m+p} - T_p}, & m \geq 1, n \geq 0. \end{cases} \quad (50)$$

Then,

$$D_{n,m,p} = \begin{cases} \sum_{p \leq i_1 \leq i_2 \leq \dots \leq i_{n-m} \leq m+p} \prod_{k=1}^{n-m} T_{i_k}, & 0 \leq m < n, \\ 1, & m = n, \\ 0, & m > n. \end{cases} \quad (51)$$

Among them,  $\forall a \in \mathbb{R}$ ,  $a^0 = 0$  is conventionally defined. Specifically, for cases where  $0 < m \leq n$ ,

$$D_{n,m,p} = \sum_{k=0}^{n-m} T_p^k D_{n-k-1,m-1,p+1} = \sum_{k=0}^{n-m} T_{m+p}^k D_{n-k-1,m-1,p}. \quad (52)$$

*Proof.*  $D_{n,m,p}$  is well-defined since  $\forall p \in \mathbb{N}^*$ ,  $m \geq 1$ ,  $T_p < T_{m+p}$ . For the case where  $n=0$  or  $m=0$ , (51) holds evidently. For the case where  $0 < m = n$ , (52) holds evidently if (51) holds.

Now we prove the case where  $0 < m \leq n$  by induction. Since  $D_{n,0,p} = T_p^n$ , we have

$$\begin{aligned} D_{n,1,p} &= \frac{D_{n,0,p+1} - D_{n,0,p}}{T_{p+1} - T_p} = \frac{T_{p+1}^n - T_p^n}{T_{p+1} - T_p} = \sum_{k=0}^{n-1} T_p^k T_{p+1}^{n-1-k} = \sum_{p \leq i_1 \leq i_2 \leq \dots \leq i_{n-1} \leq p+1} \prod_{k=1}^{n-1} T_{i_k} \\ &= \sum_{k=0}^{n-1} T_p^k D_{n-k-1,0,p+1} = \sum_{k=0}^{n-1} T_{p+1}^k D_{n-k-1,0,p}. \end{aligned} \quad (53)$$

Therefore, (51) and (52) hold for  $1 = m \leq n$ .

Assume that (51) and (52) hold for  $m \leq M$ ,  $n \geq m$ ,  $M \geq 1$ . Consider the case where  $n = m = M + 1$ .  $D_{M+1,M,p} = \sum_{p \leq i \leq M+p} T_i = \sum_{i=p}^{M+p} T_i$ . Hence,

$$D_{M+1,M+1,p} = \frac{D_{M+1,M,p+1} - D_{M+1,M,p}}{T_{p+M+1} - T_p} = \frac{\sum_{i=p+1}^{M+p+1} T_i - \sum_{i=p}^{M+p} T_i}{T_{p+M+1} - T_p} = 1. \quad (54)$$

Therefore, (51) and (52) hold for  $n = m = M + 1$ .

Consider the case where  $n > m = M + 1$ . Note that  $n > m - 1 = M$ , so

$$\begin{aligned} D_{n,M+1,p} &= \frac{D_{n,M,p+1} - D_{n,M,p}}{T_{p+M+1} - T_p} \\ &= \frac{\sum_{k=0}^{n-M} T_{p+M+1}^k D_{n-k-1,M-1,p+1} - \sum_{k=0}^{n-M} T_p^k D_{n-k-1,M-1,p+1}}{T_{p+M+1} - T_p} = \sum_{k=0}^{n-M} \frac{T_{p+M+1}^k - T_p^k}{T_{p+M+1} - T_p} D_{n-k-1,M-1,p+1} \\ &= \sum_{k=0}^{n-M} \sum_{q=0}^{k-1} T_p^q T_{p+M+1}^{k-q-1} \sum_{p+1 \leq i_{q+1} \leq i_{q+2} \leq \dots \leq i_{n-M-k+q} \leq p+M} \prod_{j=q+1}^{n-M-k+q} T_{i_j} \\ &= \sum_{k=0}^{n-M} \sum_{q=0}^{k-1} \sum_{\substack{i_1=i_2=\dots=i_q=p \\ p+1 \leq i_{q+1} \leq i_{q+2} \leq \dots \leq i_{n-M-k+q} \leq p+M \\ i_{n-M-k+q+1}=i_{n-M-k+q+1}=\dots=i_{n-M-1}=p+M+1}} \prod_{j=1}^{n-M-1} T_{i_j} \\ &= \sum_{p \leq i_1 \leq i_2 \leq \dots \leq i_{n-M-1} \leq p+M+1} \prod_{j=1}^{n-M-1} T_{i_j}. \end{aligned} \quad (55)$$

Therefore, (51) holds for  $n > m = M + 1$ , implying (52). By induction, Lemma 4 holds.  $\square$

*Proof of Theorem 8.* In this proof, we denote  $\mathbf{A} \leftrightarrow \mathbf{B}$  if  $\mathbf{A}$  has full row rank if and only if  $\mathbf{B}$  has full row rank.

Denote  $\mathbf{x} = \mathbf{x}^{(i)}(t)$ ,  $i = 1, 2, \dots, N$ , as the solution of the initial value problem

$$\begin{cases} \dot{x}_1(t) = 0, t \in \mathbb{R}, \\ \dot{x}_{k+1}(t) = x_k(t), k = 1, 2, \dots, n-1, t \in \mathbb{R}, \\ \mathbf{x} \left( \sum_{j=1}^i t_j^* \right) = \mathbf{x}_{i,0:(n-1)}^*. \end{cases}$$

Then, according to Lemma 2,

$$\begin{aligned} \mathbf{J} &\leftrightarrow \begin{bmatrix} \Phi_n^{-1}(t_1^*) & & & & \\ & \Phi_n^{-1}(t_2^*) & & & \\ & & \ddots & & \\ & & & \Phi_n^{-1}(t_N^*) & \\ & & & & \mathbf{I}_{\sum_{i=1}^{N-1} |s_i|} \end{bmatrix} \mathbf{J} \\ &\leftrightarrow \begin{bmatrix} \mathbf{I}_n & -\Phi_n(-t_1^*) & & & & \mathbf{x}^{(1)}(0) & & \\ & \mathbf{I}_n & -\Phi_n(-t_2^*) & & & & \mathbf{x}^{(2)}(t_1^*) & \\ & & \ddots & \ddots & & & & \ddots \\ & & & \mathbf{I}_n & -\Phi_n(-t_{N-1}^*) & & & \mathbf{x}^{(N-1)} \left( \sum_{i=1}^{N-2} t_i^* \right) \\ & & & & \mathbf{I}_n & & & \mathbf{x}^{(N)} \left( \sum_{i=1}^{N-1} t_i^* \right) \\ & \mathbf{I}_{|s_1| \times n} & & & & & & \\ & & \mathbf{I}_{|s_2| \times n} & & & & & \\ & & & \ddots & & & & \\ & & & & \mathbf{I}_{|s_{N-1}| \times n} & & & \end{bmatrix}. \end{aligned}$$

Upon left multiplication by

$$\prod_{i=1}^{N-1} \begin{bmatrix} \mathbf{I}_{(i-1)n} & & & \\ & \mathbf{I}_n & \Phi_n(-t_i^*) & \\ & & \mathbf{I}_n & \\ & & & \mathbf{I}_{(N-i-1)n + \sum_{i=1}^{N-1} |s_i|} \end{bmatrix},$$

we have

$$\mathbf{J} \leftrightarrow \begin{bmatrix} \mathbf{I}_n & & & \mathbf{x}^{(1)}(0) & \mathbf{x}^{(2)}(0) & \cdots & \mathbf{x}^{(N)}(0) \\ & \mathbf{I}_n & & \mathbf{x}^{(2)}(t_1) & \cdots & & \mathbf{x}^{(N)}(t_1) \\ & & \ddots & & & \ddots & \vdots \\ & & & \mathbf{I}_n & & & \mathbf{x}^{(N)}\left(\sum_{i=1}^{N-1} t_i\right) \\ & \mathbf{I}_{|s_1| \times n} & & & & & \\ & & \ddots & & & & \\ & & & \mathbf{I}_{|s_{N-1}| \times n} & & & \end{bmatrix}.$$

Upon left multiplication by

$$\begin{bmatrix} \Phi_n\left(\sum_{i=1}^N t_i^*\right) & & & & & & \\ & \Phi_n\left(\sum_{i=2}^N t_i^*\right) & & & & & \\ & & \ddots & & & & \\ & & & \Phi_n(t_N^*) & & & \\ & & & & \mathbf{I}_{\sum_{i=1}^{N-1} |s_i|} & & \end{bmatrix},$$

since  $t_f^* = \sum_{i=1}^N t_i^*$ , we have

$$\mathbf{J} \leftrightarrow \begin{bmatrix} \Phi_n\left(\sum_{i=1}^N t_i^*\right) & & & \mathbf{x}^{(1)}(t_f^*) & \mathbf{x}^{(2)}(t_f^*) & \cdots & \mathbf{x}^{(N)}(t_f^*) \\ & \Phi_n\left(\sum_{i=2}^N t_i^*\right) & & \mathbf{x}^{(2)}(t_f^*) & \cdots & \mathbf{x}^{(N)}(t_f^*) & \\ & & \ddots & & & \ddots & \vdots \\ & & & \Phi_n(t_N^*) & & & \mathbf{x}^{(N)}(t_f^*) \\ & \mathbf{I}_{|s_1| \times n} & & & & & \\ & & \ddots & & & & \\ & & & \mathbf{I}_{|s_{N-1}| \times n} & & & \end{bmatrix}.$$

According to Lemma 2.3,  $\forall a \in \mathbb{N}^*$ ,  $t \in \mathbb{R}$ ,  $\Phi_a(t)$  is invertible. Eliminate the first  $n$  rows and the first  $n$  columns of  $\mathbf{J}$ , we have

$$\mathbf{J} \leftrightarrow \begin{bmatrix} \Phi_n\left(\sum_{i=2}^N t_i^*\right) & & & \mathbf{x}^{(2)}(t_f^*) & \mathbf{x}^{(3)}(t_f^*) & \cdots & \mathbf{x}^{(N)}(t_f^*) \\ & \Phi_n\left(\sum_{i=3}^N t_i^*\right) & & \mathbf{x}^{(3)}(t_f^*) & \cdots & \mathbf{x}^{(N)}(t_f^*) & \\ & & \ddots & & & \ddots & \vdots \\ & & & \Phi_n(t_N^*) & & & \mathbf{x}^{(N)}(t_f^*) \\ \mathbf{I}_{|s_1| \times n} & & & & & & \\ & \mathbf{I}_{|s_2| \times n} & & & & & \\ & & \ddots & & & & \\ & & & \mathbf{I}_{|s_{N-1}| \times n} & & & \end{bmatrix}.$$

For each  $\mathbf{I}_{|s_i| \times n} = \begin{bmatrix} \mathbf{I}_{|s_i|} & \mathbf{0}_{|s_i| \times (n-|s_i|)} \end{bmatrix}$ ,  $i = 1, 2, \dots, N-1$ , eliminate the rows and columns occupied by  $\mathbf{I}_{|s_i|}$ . Then,

$$\mathbf{J} \leftrightarrow \begin{bmatrix} \mathbf{0}_{|s_1| \times (n-|s_1|)} & & & \mathbf{x}_{1:|s_1|}^{(2)}(t_f^*) & \mathbf{x}_{1:|s_1|}^{(3)}(t_f^*) & \cdots & \mathbf{x}_{1:|s_1|}^{(N)}(t_f^*) \\ \Phi_{n-|s_1|}\left(\sum_{i=2}^N t_i^*\right) & & & \mathbf{x}_{(|s_1|+1):n}^{(2)}(t_f^*) & \mathbf{x}_{(|s_1|+1):n}^{(3)}(t_f^*) & \cdots & \mathbf{x}_{(|s_1|+1):n}^{(N)}(t_f^*) \\ & \mathbf{0}_{|s_2| \times (n-|s_2|)} & & \mathbf{x}_{1:|s_2|}^{(3)}(t_f^*) & \cdots & \mathbf{x}_{1:|s_2|}^{(N)}(t_f^*) \\ & \Phi_{n-|s_2|}\left(\sum_{i=3}^N t_i^*\right) & & \mathbf{x}_{(|s_2|+1):n}^{(3)}(t_f^*) & \cdots & \mathbf{x}_{(|s_2|+1):n}^{(N)}(t_f^*) \\ & & \ddots & & & \ddots & \vdots \\ & & & \mathbf{0}_{|s_{N-1}| \times (n-|s_{N-1}|)} & & & \mathbf{x}_{1:|s_{N-1}|}^{(N)}(t_f^*) \\ & & & \Phi_{n-|s_{N-1}|}(t_N^*) & & & \mathbf{x}_{(|s_{N-1}|+1):n}^{(N)}(t_f^*) \end{bmatrix}.$$

Eliminate the rows and columns occupied by  $\Phi_{n-|s_i|} \left( \sum_{j=i+1}^N t_j^* \right)$ ,  $\forall i = 1, 2, \dots, N-1$ . Then,  $\mathbf{J} \leftrightarrow \mathbf{J}_1$ , where

$$\mathbf{J}_1 = \begin{bmatrix} \mathbf{x}_{1:|s_1|}^{(2)}(t_f^*) & \mathbf{x}_{1:|s_1|}^{(3)}(t_f^*) & \cdots & \mathbf{x}_{1:|s_1|}^{(N)}(t_f^*) \\ & \mathbf{x}_{1:|s_2|}^{(3)}(t_f^*) & \cdots & \mathbf{x}_{1:|s_2|}^{(N)}(t_f^*) \\ & & \ddots & \vdots \\ & & & \mathbf{x}_{1:|s_{N-1}|}^{(N)}(t_f^*) \end{bmatrix}. \quad (56)$$

Next we prove  $\mathbf{J}$  in (56) has full row rank. If  $\forall i = 1, 2, \dots, N-1$ ,  $|s_i| = 0$ , then  $\text{rank} \mathbf{J} = Nn = Nn + \sum_{i=1}^{N-1} |s_i|$ . In this case,  $\mathbf{J}$  has full row rank. We consider the case where  $\exists i = 1, 2, \dots, N-1$ ,  $|s_i| \neq 0$  in the following. Assume  $1 \leq i_1 < i_2 < \dots < i_{N'} \leq N-1$ , s.t.

$$\begin{cases} |s_i| \neq 0, & \text{if } i \in \{i_j\}_{j=1}^{N'}, \\ |s_i| = 0, & \text{otherwise.} \end{cases}$$

Then, (56) can be rewritten as

$$\mathbf{J}_2 = \begin{bmatrix} \mathbf{x}_{1:|s_{i_1}|}^{(i_1+1)}(t_f^*) & \mathbf{x}_{1:|s_{i_1}|}^{(i_1+2)}(t_f^*) & \cdots & \mathbf{x}_{1:|s_{i_1}|}^{(i_2)}(t_f^*) & \mathbf{x}_{1:|s_{i_1}|}^{(i_2+1)}(t_f^*) & \mathbf{x}_{1:|s_{i_1}|}^{(i_2+2)}(t_f^*) & \cdots & \mathbf{x}_{1:|s_{i_1}|}^{(i_{N'})}(t_f^*) & \mathbf{x}_{1:|s_{i_1}|}^{(i_{N'}+1)}(t_f^*) & \mathbf{x}_{1:|s_{i_1}|}^{(i_{N'}+2)}(t_f^*) & \cdots & \mathbf{x}_{1:|s_{i_1}|}^{(N)}(t_f^*) \\ & & & \mathbf{x}_{1:|s_{i_2}|}^{(i_2+1)}(t_f^*) & \mathbf{x}_{1:|s_{i_2}|}^{(i_2+2)}(t_f^*) & \cdots & \mathbf{x}_{1:|s_{i_2}|}^{(i_{N'})}(t_f^*) & \mathbf{x}_{1:|s_{i_2}|}^{(i_{N'}+1)}(t_f^*) & \mathbf{x}_{1:|s_{i_2}|}^{(i_{N'}+2)}(t_f^*) & \cdots & \mathbf{x}_{1:|s_{i_2}|}^{(N)}(t_f^*) \\ & & & & \ddots & \ddots & & \vdots & \vdots & \ddots & \vdots \\ & & & & & & \mathbf{x}_{1:|s_{i_{N'}}|}^{(i_{N'}+1)}(t_f^*) & \mathbf{x}_{1:|s_{i_{N'}}|}^{(i_{N'}+2)}(t_f^*) & \cdots & \mathbf{x}_{1:|s_{i_{N'}}|}^{(N)}(t_f^*) \end{bmatrix}, \quad (57)$$

where  $\mathbf{J} \leftrightarrow \mathbf{J}_1 \leftrightarrow \mathbf{J}_2$ .

According to (44a),  $\forall i = 1, 2, \dots, N$ ,  $k = 1, 2, \dots, n$ ,  $x_{i,k}^* = \sum_{j=1}^k \frac{1}{(k-j)!} x_{i-1,j}^* t_i^{*k-j} + \frac{1}{k!} u_i t_i^{*k}$ . So  $x_{i-1,k}^* = \sum_{j=1}^k \frac{1}{(k-j)!} x_{i,j}^* (-t_i^*)^{k-j} + \frac{1}{k!} u_i (-t_i^*)^k$ .

In other words,

$$x_k^{(i-1)} \left( \sum_{j=1}^{i-1} t_j^* \right) = \sum_{j=1}^k \frac{(-t_i^*)^{k-j}}{(k-j)!} x_k^{(i)} \left( \sum_{j=1}^i t_j^* \right), \quad \forall i = 1, 2, \dots, N, \quad k = 2, 3, \dots, n.$$

So  $\forall i = 1, 2, \dots, N$ ,

$$\begin{aligned} \mathbf{x}^{(i)} \left( \sum_{j=1}^{i-1} t_j^* \right) &= \Phi_n(-t_i^*) \mathbf{x}^{(i)} \left( \sum_{j=1}^i t_j^* \right) = \begin{bmatrix} x_1^{(i)} \left( \sum_{j=1}^i t_j^* \right) \\ \mathbf{x}_{2:n}^{(i-1)} \left( \sum_{j=1}^{i-1} t_j^* \right) \end{bmatrix} \\ &= \mathbf{x}^{(i-1)} \left( \sum_{j=1}^{i-1} t_j^* \right) + \left( x_1^{(i)} \left( \sum_{j=1}^i t_j^* \right) - x_1^{(i-1)} \left( \sum_{j=1}^{i-1} t_j^* \right) \right) \mathbf{e}_1. \end{aligned}$$

In other words,  $\forall i = 1, 2, \dots, N$ ,

$$\mathbf{x}^{(i)} \left( \sum_{j=1}^{i-1} t_j^* \right) - \mathbf{x}^{(i-1)} \left( \sum_{j=1}^{i-1} t_j^* \right) = \Delta u_i \mathbf{e}_1 = \Delta u_i \phi_n(0), \quad (58)$$

where  $\Delta u_i \triangleq x_1^{(i)} \left( \sum_{j=1}^i t_j^* \right) - x_1^{(i-1)} \left( \sum_{j=1}^{i-1} t_j^* \right) = u_i - u_{i-1} \neq 0$ ,  $\forall i = 2, 3, \dots, N$ , since  $u_i$  and  $u_{i-1}$  are the control of the different stages  $s_i$  and  $s_{i-1}$ , respectively. Specifically, if  $|s_i| \neq 0$ , then  $u_i = 0$ , and  $\mathbf{x}_{1:|s_i|}^{(i-1)} \left( \sum_{j=1}^i t_j^* \right) = \mathbf{0}_{|s_i| \times 1}$ ; hence

$$\mathbf{x}^{(i+1)} \left( \sum_{j=1}^i t_j^* \right) = u_i \phi_n(0), \quad |s_i| \neq 0. \quad (59)$$

According to (58), (59), and Lemma 2, let

$$\begin{aligned} & \mathbf{J}_3 \\ &= \left( \prod_{j=i_1+1}^N \begin{bmatrix} \Phi_{|s_{i_1}|}(-t_j) & & & \\ & \Phi_{|s_{i_2}|}(-t_j) & & \\ & & \ddots & \\ & & & \Phi_{|s_{i_{N'}}|}(-t_j) \end{bmatrix} \right) \mathbf{J}_2 \left( \prod_{j=i_1+1}^{N-1} \begin{bmatrix} \mathbf{I}_{N-1-j} & 1 & -1 \\ & 1 & \\ & & \mathbf{I}_{j-i_1-1} \end{bmatrix} \right) \begin{bmatrix} \frac{1}{\Delta u_{i_1+1}} & & & \\ & \frac{1}{\Delta u_{i_1+2}} & & \\ & & \ddots & \\ & & & \frac{1}{\Delta u_N} \end{bmatrix} \\ &= \begin{bmatrix} \phi_{|s_{i_1}|}(-T_{i_1+1}) & \phi_{|s_{i_1}|}(-T_{i_1+2}) & \cdots & \phi_{|s_{i_1}|}(-T_{i_2}) & \phi_{|s_{i_1}|}(-T_{i_2+1}) & \phi_{|s_{i_1}|}(-T_{i_2+2}) & \cdots & \phi_{|s_{i_1}|}(-T_{i_{N'}+1}) & \phi_{|s_{i_1}|}(-T_{i_{N'}+2}) & \cdots & \phi_{|s_{i_1}|}(-T_N) \\ \phi_{|s_{i_2}|}(-T_{i_2+1}) & \phi_{|s_{i_2}|}(-T_{i_2+2}) & \cdots & \phi_{|s_{i_2}|}(-T_{i_{N'}}) & \phi_{|s_{i_2}|}(-T_{i_{N'}+1}) & \phi_{|s_{i_2}|}(-T_{i_{N'}+2}) & \cdots & \phi_{|s_{i_2}|}(-T_N) & & & \\ & & \ddots & & & & \ddots & & & & \\ & & & & & & & \phi_{|s_{i_{N'}}|}(-T_{i_{N'}+1}) & \phi_{|s_{i_{N'}}|}(-T_{i_{N'}+2}) & \cdots & \phi_{|s_{i_{N'}}|}(-T_N) \end{bmatrix} \end{aligned} \quad (60)$$



where  $T_i = \sum_{j=i_1+1}^{i-1} t_j^*$ . It is evidently that  $\mathbf{J} \leftrightarrow \mathbf{J}_2 \leftrightarrow \mathbf{J}_3$ . Note that (60) successfully avoid the complex background of the time-optimal problem. Left-multiplying matrix  $\mathbf{J}_3$  by

$$\begin{bmatrix} \text{diag} \left( \left( (-1)^{j-1} (j-1)! \right)_{j=1}^{|s_{i_1}|} \right) & & & \\ & \text{diag} \left( \left( (-1)^{j-1} (j-1)! \right)_{j=1}^{|s_{i_2}|} \right) & & \\ & & \ddots & \\ & & & \text{diag} \left( \left( (-1)^{j-1} (j-1)! \right)_{j=1}^{|s_{i_{N'}}|} \right) \end{bmatrix},$$

we have  $\mathbf{J} \leftrightarrow \mathbf{J}_3 \leftrightarrow \mathbf{J}_4$ , where

$$\mathbf{J}_4 = \begin{bmatrix} \hat{\phi}_{|s_{i_1}|}(T_{i_1+1}) & \hat{\phi}_{|s_{i_1}|}(T_{i_1+2}) & \cdots & \hat{\phi}_{|s_{i_1}|}(T_{i_2}) & \hat{\phi}_{|s_{i_1}|}(T_{i_2+1}) & \hat{\phi}_{|s_{i_1}|}(T_{i_2+2}) & \cdots & \hat{\phi}_{|s_{i_1}|}(T_{i_{N'}}) & \hat{\phi}_{|s_{i_1}|}(T_{i_{N'}+1}) & \hat{\phi}_{|s_{i_1}|}(T_{i_{N'}+2}) & \cdots & \hat{\phi}_{|s_{i_1}|}(T_N) \\ & \hat{\phi}_{|s_{i_2}|}(T_{i_2+1}) & \hat{\phi}_{|s_{i_2}|}(T_{i_2+2}) & \cdots & \hat{\phi}_{|s_{i_2}|}(T_{i_{N'}}) & \hat{\phi}_{|s_{i_2}|}(T_{i_{N'}+1}) & \hat{\phi}_{|s_{i_2}|}(T_{i_{N'}+2}) & \cdots & \hat{\phi}_{|s_{i_2}|}(T_N) & & & \\ & & & \ddots & & & & \ddots & & & & \\ & & & & & & & & \hat{\phi}_{|s_{i_{N'}}|}(T_{i_{N'}+1}) & \hat{\phi}_{|s_{i_{N'}}|}(T_{i_{N'}+2}) & \cdots & \hat{\phi}_{|s_{i_{N'}}|}(T_N) \end{bmatrix}. \quad (61)$$

In (61),  $T_{i_1+1} < T_{i_1+2} < \cdots < T_N$ , since  $\forall i = 1, 2, \dots, N$ ,  $t_i > 0$ .  $\mathbf{J}_4$  in (61) has a form similar to the Vandermonde matrix. Now, we only need to proof that  $\mathbf{J}_4$  has full row rank based on Lemma 4.

Denote  $\mathbf{D}_{m,p}^{a:b} \triangleq (D_{l,m,p})_{l=a}^b$ , where  $D_{l,m,p} = D_{l,m} \left( (T_k)_{k=p}^{m+p} \right)$  is defined in (50). Then,  $\hat{\phi}_l(T_p) = D_{0,p}^{0:(l-1)}$ . Therefore,

$$\mathbf{J}_4 = \begin{bmatrix} D_{0,i_1+1}^{0:(|s_{i_1}|-1)} & D_{0,i_1+2}^{0:(|s_{i_1}|-1)} & \cdots & D_{0,i_2}^{0:(|s_{i_1}|-1)} & D_{0,i_2+1}^{0:(|s_{i_1}|-1)} & D_{0,i_2+2}^{0:(|s_{i_1}|-1)} & \cdots & D_{0,i_{N'}}^{0:(|s_{i_1}|-1)} & D_{0,i_{N'}+1}^{0:(|s_{i_1}|-1)} & D_{0,i_{N'}+2}^{0:(|s_{i_1}|-1)} & \cdots & D_{0,N}^{0:(|s_{i_1}|-1)} \\ & D_{0,i_2+1}^{0:(|s_{i_2}|-1)} & D_{0,i_2+2}^{0:(|s_{i_2}|-1)} & \cdots & D_{0,i_{N'}}^{0:(|s_{i_2}|-1)} & D_{0,i_{N'}+1}^{0:(|s_{i_2}|-1)} & D_{0,i_{N'}+2}^{0:(|s_{i_2}|-1)} & \cdots & D_{0,N}^{0:(|s_{i_2}|-1)} & & & \\ & & & \ddots & & & & \ddots & & & & \\ & & & & & & & & D_{0,i_{N'}+1}^{0:(|s_{i_{N'}}|-1)} & D_{0,i_{N'}+2}^{0:(|s_{i_{N'}}|-1)} & \cdots & D_{0,N}^{0:(|s_{i_{N'}}|-1)} \end{bmatrix}. \quad (62)$$

We prove  $\mathbf{J}_4$  has full row rank through row operations. At each step, we first subtract the preceding column from the succeeding one and then divide by the corresponding time difference. Take the first step as example:

$$\begin{aligned} & \mathbf{J} \leftrightarrow \mathbf{J}_4 \\ & = \begin{bmatrix} 1 & 1 & \cdots & 1 & 1 & 1 & \cdots & 1 & 1 & 1 & \cdots & 1 \\ D_{0,i_1+1}^{1:(|s_{i_1}|-1)} & D_{0,i_1+2}^{1:(|s_{i_1}|-1)} & \cdots & D_{0,i_2}^{1:(|s_{i_1}|-1)} & D_{0,i_2+1}^{1:(|s_{i_1}|-1)} & D_{0,i_2+2}^{1:(|s_{i_1}|-1)} & \cdots & D_{0,i_{N'}}^{1:(|s_{i_1}|-1)} & D_{0,i_{N'}+1}^{1:(|s_{i_1}|-1)} & D_{0,i_{N'}+2}^{1:(|s_{i_1}|-1)} & \cdots & D_{0,N}^{1:(|s_{i_1}|-1)} \\ & 1 & 1 & \cdots & 1 & 1 & \cdots & 1 & 1 & 1 & \cdots & 1 \\ & D_{0,i_2+1}^{1:(|s_{i_2}|-1)} & D_{0,i_2+2}^{1:(|s_{i_2}|-1)} & \cdots & D_{0,i_{N'}}^{1:(|s_{i_2}|-1)} & D_{0,i_{N'}+1}^{1:(|s_{i_2}|-1)} & D_{0,i_{N'}+2}^{1:(|s_{i_2}|-1)} & \cdots & D_{0,N}^{1:(|s_{i_2}|-1)} & & & \\ & & & \ddots & & & & \ddots & & & & \\ & & & & & & & & 1 & 1 & \cdots & 1 \\ & & & & & & & & D_{0,i_{N'}+1}^{1:(|s_{i_{N'}}|-1)} & D_{0,i_{N'}+2}^{1:(|s_{i_{N'}}|-1)} & \cdots & D_{0,N}^{1:(|s_{i_{N'}}|-1)} \end{bmatrix} \\ & \leftrightarrow \begin{bmatrix} 1 & 0 & \cdots & 0 & 0 & 0 & \cdots & 0 & 0 & 0 & \cdots & 0 \\ D_{0,i_1+1}^{1:(|s_{i_1}|-1)} & D_{1,i_1+1}^{1:(|s_{i_1}|-1)} & \cdots & D_{1,i_2-1}^{1:(|s_{i_1}|-1)} & D_{1,i_2}^{1:(|s_{i_1}|-1)} & D_{1,i_2+1}^{1:(|s_{i_1}|-1)} & \cdots & D_{1,i_{N'}-1}^{1:(|s_{i_1}|-1)} & D_{1,i_{N'}}^{1:(|s_{i_1}|-1)} & D_{1,i_{N'}+1}^{1:(|s_{i_1}|-1)} & \cdots & D_{1,N-1}^{1:(|s_{i_1}|-1)} \\ & 1 & 0 & \cdots & 0 & 0 & \cdots & 0 & 0 & 0 & \cdots & 0 \\ & D_{0,i_2+1}^{1:(|s_{i_2}|-1)} & D_{1,i_2+1}^{1:(|s_{i_2}|-1)} & \cdots & D_{1,i_{N'}-1}^{1:(|s_{i_2}|-1)} & D_{1,i_{N'}}^{1:(|s_{i_2}|-1)} & D_{1,i_{N'}+1}^{1:(|s_{i_2}|-1)} & \cdots & D_{1,N-1}^{1:(|s_{i_2}|-1)} & & & \\ & & & \ddots & & & & \ddots & & & & \\ & & & & & & & & 1 & 0 & \cdots & 0 \\ & & & & & & & & D_{0,i_{N'}+1}^{1:(|s_{i_{N'}}|-1)} & D_{1,i_{N'}+1}^{1:(|s_{i_{N'}}|-1)} & \cdots & D_{1,N-1}^{1:(|s_{i_{N'}}|-1)} \end{bmatrix} \\ & \leftrightarrow \begin{bmatrix} D_{1,i_1+1}^{1:(|s_{i_1}|-1)} & \cdots & D_{1,i_2-1}^{1:(|s_{i_1}|-1)} & D_{1,i_2+1}^{1:(|s_{i_1}|-1)} & \cdots & D_{1,i_{N'}-1}^{1:(|s_{i_1}|-1)} & D_{1,i_{N'}}^{1:(|s_{i_1}|-1)} & \cdots & D_{1,N-1}^{1:(|s_{i_1}|-1)} \\ & & D_{1,i_2+1}^{1:(|s_{i_2}|-1)} & \cdots & D_{1,i_{N'}-1}^{1:(|s_{i_2}|-1)} & D_{1,i_{N'}}^{1:(|s_{i_2}|-1)} & \cdots & D_{1,N-1}^{1:(|s_{i_2}|-1)} \\ & & & \ddots & & & & \ddots & \\ & & & & & & & & D_{1,i_{N'}+1}^{1:(|s_{i_{N'}}|-1)} & \cdots & D_{1,N-1}^{1:(|s_{i_{N'}}|-1)} \end{bmatrix}. \end{aligned}$$

At the second step, elements  $D_{1,i_j}^{1:(|s_{i_l}|-1)}$  does not exist. Fortunately, the difference between  $D_{1,i_j}^{1:(|s_{i_l}|\pm 1)}$  can be eliminated,

resulting in a matrix with similar structures to the above one. At the second step, it is noteworthy that  $D_{1,1,p} = 1$ . Then,

$$\begin{aligned}
 & \begin{matrix} J \\ \leftrightarrow \\ \leftrightarrow \\ \leftrightarrow \end{matrix} \left[ \begin{array}{cccccccccccccccc}
 1 & 1 & \cdots & 1 & 1 & 1 & \cdots & 1 & 1 & 1 & \cdots & 1 \\
 D_{1,i_1+1}^{2:(|s_{i_1}|-1)} & D_{1,i_1+2}^{2:(|s_{i_1}|-1)} & \cdots & D_{1,i_2-1}^{2:(|s_{i_1}|-1)} & D_{1,i_2+1}^{2:(|s_{i_1}|-1)} & D_{1,i_2+2}^{2:(|s_{i_1}|-1)} & \cdots & D_{1,i_{N'}-1}^{2:(|s_{i_1}|-1)} & D_{1,i_{N'}+1}^{2:(|s_{i_1}|-1)} & D_{1,i_{N'}+2}^{2:(|s_{i_1}|-1)} & \cdots & D_{1,N-1}^{2:(|s_{i_1}|-1)} \\
 & & & & 1 & 1 & \cdots & 1 & 1 & 1 & \cdots & 1 \\
 & & & D_{1,i_2+1}^{2:(|s_{i_2}|-1)} & D_{1,i_2+2}^{2:(|s_{i_2}|-1)} & \cdots & D_{1,i_{N'}-1}^{2:(|s_{i_2}|-1)} & D_{1,i_{N'}+1}^{2:(|s_{i_2}|-1)} & D_{1,i_{N'}+2}^{2:(|s_{i_2}|-1)} & \cdots & D_{1,N-1}^{2:(|s_{i_2}|-1)} \\
 & & & & & & \ddots & \ddots & \vdots & \vdots & \ddots & \vdots \\
 & & & & & & & & 1 & 1 & \cdots & 1 \\
 & & & & & & & & D_{1,i_{N'}+1}^{2:(|s_{i_{N'}}|-1)} & D_{1,i_{N'}+2}^{2:(|s_{i_{N'}}|-1)} & \cdots & D_{1,N-1}^{2:(|s_{i_{N'}}|-1)} \\
 1 & 0 & \cdots & 0 & 0 & 0 & \cdots & 0 & 0 & 0 & \cdots & 0 \\
 D_{1,i_1+1}^{2:(|s_{i_1}|-1)} & D_{2,i_1+1}^{2:(|s_{i_1}|-1)} & \cdots & D_{2,i_2-2}^{2:(|s_{i_1}|-1)} & * & D_{2,i_2+1}^{2:(|s_{i_1}|-1)} & \cdots & D_{2,i_{N'}-2}^{2:(|s_{i_1}|-1)} & * & D_{2,i_{N'}+1}^{2:(|s_{i_1}|-1)} & \cdots & D_{2,N-2}^{2:(|s_{i_1}|-1)} \\
 & & & & 1 & 0 & \cdots & 0 & 0 & 0 & \cdots & 0 \\
 & & & D_{1,i_2+1}^{2:(|s_{i_2}|-1)} & D_{2,i_2+1}^{2:(|s_{i_2}|-1)} & \cdots & D_{2,i_{N'}-2}^{2:(|s_{i_2}|-1)} & * & D_{2,i_{N'}+1}^{2:(|s_{i_2}|-1)} & \cdots & D_{2,N-2}^{2:(|s_{i_2}|-1)} \\
 & & & & & & \ddots & \ddots & \vdots & \vdots & \ddots & \vdots \\
 & & & & & & & & 1 & 0 & \cdots & 0 \\
 & & & & & & & & D_{1,i_{N'}+1}^{2:(|s_{i_{N'}}|-1)} & D_{2,i_{N'}+1}^{2:(|s_{i_{N'}}|-1)} & \cdots & D_{2,N-2}^{2:(|s_{i_{N'}}|-1)} \\
 D_{2,i_1+1}^{2:(|s_{i_1}|-1)} & \cdots & D_{2,i_2-2}^{2:(|s_{i_1}|-1)} & D_{2,i_2+1}^{2:(|s_{i_1}|-1)} & \cdots & D_{2,i_{N'}-2}^{2:(|s_{i_1}|-1)} & D_{2,i_{N'}+1}^{2:(|s_{i_1}|-1)} & \cdots & D_{2,N-2}^{2:(|s_{i_1}|-1)} \\
 & & & D_{2,i_2+1}^{2:(|s_{i_2}|-1)} & \cdots & D_{2,i_{N'}-2}^{2:(|s_{i_2}|-1)} & D_{2,i_{N'}+1}^{2:(|s_{i_2}|-1)} & \cdots & D_{2,N-2}^{2:(|s_{i_2}|-1)} \\
 & & & & & \ddots & \ddots & \vdots & \ddots & \vdots \\
 & & & & & & D_{2,i_{N'}+1}^{2:(|s_{i_{N'}}|-1)} & \cdots & D_{2,N-2}^{2:(|s_{i_{N'}}|-1)}
 \end{array} \right].
 \end{aligned}$$

It can be proved by Condition 1 that the above process can be continued until the last step, i.e., the matrix is empty. Therefore,  $J$  has full row rank. Theorem 8 holds.  $\square$

**Theorem 9.** *If Condition 1 holds, then the switching law  $S$  induces a manifold of  $\dim S = N - \sum_{i=1}^N |s_i|$  dimension.*

*Proof.* At  $X^*$ ,  $f(X^*) = 0$ . Theorem 8 implies that  $J^* = \frac{df}{dX} \Big|_{X^*} = (j_1^*, j_2^*, \dots, j_{N(n+1)}^*)$  has full row rank, i.e.,  $\text{rank } J^* = Nn + \sum_{i=1}^N |s_i|$ . Assume that  $\{j_{i_k}^*\}_{k=1}^{\text{rank } J^*}$  are linearly independent. Denote  $\{i_k'\}_{k=1}^{N(n+1)-\text{rank } J^*} = \{k\}_{k=1}^{N(n+1)} \setminus \{j_{i_k}^*\}_{k=1}^{\text{rank } J^*}$ . Applying the implicit function theorem,  $f(X) = 0$  induces a smooth map

$$\hat{f} : \left( X_{i_k'} \right)_{k=1}^{N(n+1)-\text{rank } J^*} \mapsto (X_{i_k})_{k=1}^{\text{rank } J^*}$$

near  $X^*$ . Therefore, the map of the smooth function  $\hat{f}$ , i.e., the set induced by  $f(X) = 0$  near  $X^*$ , is a manifold of dimension  $N(n+1) - \text{rank } J^* = N - \sum_{i=1}^N |s_i|$ . The theorem holds.  $\square$